Applied Catalysis B: Environment and Energy 345 (2024) 123676

Contents lists available at ScienceDirect

Applied Catalysis B: Environment and Energy

journal homepage: www.elsevier.com/locate/apcatb

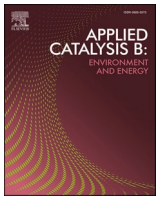

Carbon-free fuels for direct liquid-feed fuel cells: Anodic electrocatalysts and influence of the experimental conditions on the reaction kinetics and mechanisms

Evgeniia A. Vorms [a], Alexandr G. Oshchepkov [a], Antoine Bonnefont [b], Elena R. Savinova [a], Marian Chatenet [b,*]

[a] Institut de Chimie et Procédés pour l'Energie, l'Environnement et la Santé, UMR 7515 CNRS, University of Strasbourg, 67087 Strasbourg Cedex, France
[b] University Grenoble Alpes, University Savoie Mont Blanc, CNRS, Grenoble INP (Institute of Engineering, University Grenoble Alpes), LEPMI, 38000 Grenoble, France

ARTICLE INFO

Keywords:
Sodium borohydride
Ammonia-borane
Hydrazine
Non-carbon fuels oxidation reaction
Alkaline fuel cells

ABSTRACT

Direct fuel cells fed with liquid carbon-free fuels (borohydride, ammonia-borane, hydrazine) present a number of benefits compared to state-of-the-art proton-exchange membrane fuel cells, among them ease of fuel transportation and distribution, high volumetric energy density, high theoretical cell voltage, and number of transferred electrons $n > 2$. However, taking full advantage of these benefits requires highly active anodic catalysts, which allow efficient fuel valorization at close-to-equilibrium potentials. This requires understanding the complex mechanisms of the multi-electron fuel oxidation reactions and the main factors affecting reaction rates and product selectivities. This review offers a state-of-the-art understanding of borohydride, ammonia-borane, and hydrazine oxidation on noble metal and noble metal-free catalysts both in half- and in full-cell configuration. Electrochemical data are complemented with coupled physicochemical techniques and numerical calculations to unveil the main intermediates and co-products and the influence of the different experimental factors on the reaction kinetics and mechanisms.

1. Introduction

Electrochemical energy production from carbon-free fuels has recently attracted much attention [1–6]. This review considers complex carbon-free fuels, notably borohydride, ammonia-borane, and hydrazine, that have high energy density (Table 1), can be conveniently stored, transported and distributed in solid/liquid form, and can be converted into electrical energy either in the so-called indirect or direct fuel cells. The former are fed with hydrogen produced via catalytic hydrolysis of a fuel, while the latter are directly fed with a liquid fuel (usually as an alkaline aqueous electrolyte) that is electrooxidized at the anode. The direct liquid fuel cells, which are inherently more energy-efficient, since they benefit from low (lower than hydrogen) standard potentials (hence, higher equilibrium cell voltage) and high (higher than hydrogen) number of transferred electrons (Table 1) are subject of this review paper. The performance of direct liquid fuel cells critically depends on the availability of active and stable anode catalysts capable to fully valorize the fuel, avoiding its hydrolysis. While electrooxidation of borohydride and ammonia-borane on noble metals (Pt, Pd and Au) has been widely studied, much less is known about the activity of noble metal-free catalysts. Recent years have witnessed significant progress in the understanding of electrocatalysis of borohydride, ammonia-borane, and hydrazine oxidation both on noble metal and noble metal-free catalysts, which translated in the development of direct fuel cells with interesting performance; this rendered them attractive for industrial applications, notably for portable and mobile devices, for example, in confined spaces (such as submarines) where the use of hydrogen creates safety issues. Nevertheless, building high performance direct fuel cells still faces a number of challenges, among them design of advanced anode and cathode materials/electrodes, and membranes with low fuel crossover rates.

This review is focused on anode materials; indeed, the slow kinetics of the anode reaction often limits the overall performance of direct liquid fuel cells. Thus, development of anode materials based on abundant elements and capable to efficiently catalyze full fuel oxidation (i.e. producing the theoretical number of electrons) at low overpotential is of key importance. This, in its turn, requires understanding the product speciation, the reaction kinetics and mechanisms, and their dependence

* Corresponding author.
E-mail address: Marian.Chatenet@grenoble-inp.fr (M. Chatenet).

https://doi.org/10.1016/j.apcatb.2023.123676
Received 20 October 2023; Received in revised form 22 December 2023; Accepted 28 December 2023
Available online 30 December 2023

on the structure and composition of the electrodes.

The objective of this review is to present the state-of-the-art understanding of borohydride, ammonia-borane and hydrazine oxidation on noble metal and noble metal-free catalysts, both in half- and full-cell configuration. The manuscript is structured as follows: in Section 2 half-cell studies performed in three-electrode configuration are reviewed, focusing on different types of catalytic materials (starting from the widely investigated noble metal-based catalysts and then less-studied noble metal-free materials), reaction mechanisms and kinetics. Various carbon-free fuels, including borohydride, ammonia-borane, and hydrazine, are considered and discussed sequentially. Whenever relevant, electrochemical data are corroborated with *in situ/operando* spectroscopies and DFT (density functional theory) calculations. Armed with this information, propositions to understand why some materials are good, while others are mediocre catalysts will be made. Section 3 is devoted to full-cell studies, where current-voltage characteristics and power densities of direct fuel cells are discussed, as well as their dependence on the type of anode/cathode materials and catalytic layer architecture, with a particular emphasis on noble metal-free materials. Section 4 compares borohydride, ammonia-borane, and hydrazine oxidation mechanisms, presents the pros and cons of each of these fuels, and offers an outlook regarding direct liquid carbon-free fuel cell development.

2. Reaction kinetics and mechanisms

2.1. Borohydride oxidation reaction (BOR)

Borohydride is widely used as a reducing agent in the chemical and pharmaceutical industries but is also a promising carbon-free energy carrier for niche market applications. In aqueous solution, borohydride can be converted into borate via two competing routes, either through chemical hydrolysis to produce hydrogen (1),

$$BH_4^- + 2\,H_2O \rightarrow BO_2^- + 4\,H_2 \quad (1)$$

or via direct electrochemical oxidation (yielding in theory 8 e^- per BH_4^- species):

$$BH_4^- + 8\,OH^- \rightarrow B(OH)_4^- + 8\,e^- + 4\,H_2O \quad (2)$$

($E^\circ = -0.41$ V vs. RHE, reversible hydrogen electrode).

Hydrogen produced through fuel hydrolysis (1) can be further electrochemically oxidized in a hydrogen fuel cell through the HOR (hydrogen oxidation reaction, forward reaction of Eq.(3):

$$H_2 + 2\,OH^- = 2\,H_2O + 2\,e^- \quad (3)$$

($E^\circ = 0$ V vs RHE).

Since the rate of hydrolysis significantly decreases above pH 13, direct borohydride electrochemical oxidation is performed in strongly alkaline aqueous solutions.

The BOR witnessed a renewal of interest in 1999, when Amendola et al. first demonstrated a $NaBH_4$-fed alkaline fuel cell, the so-called direct borohydride fuel cell (DBFC) [9]. Their anode catalyst was highly dispersed high-surface-area carbon silk-supported gold/platinum nanoparticles, which was found to lead to near-complete electrochemical BOR, with 6.9 electrons exchanged per BH_4^- species. Starting from this seminal study (whose purpose was not to evaluate the BOR kinetics/mechanism but rather to demonstrate the performance of a DBFC), many authors investigated noble metal-based catalysts for the BOR. Gyenge and his research group were the most active in the 2000s, as they studied bulk gold and platinum surfaces [10], and then many carbon-supported materials: Au-based alloys [11], Ag-based alloys [12], Pd-based alloys [13], Os-based alloys [14] and of course Pt-based alloys [15]. Many others followed, like Chatenet et al. (Au and Ag surfaces) [16], Simoes et al. (PdAu/C [17] and PdBi/C [18] nanoparticles), Grimmer et al. (Ru-based [19] and Pd-based catalysts [20]) and Santos et al., who focused on Au- [21], Pt- [22] and Pd-containing [23] catalysts. Although these early papers could not provide any understanding of the reaction kinetics and mechanisms, owing to the lack of coupled physicochemical studies, they demonstrated fast BOR kinetics on Pt, and slow on Au, Pd being the only other noble metal of interest for the BOR.

Subsequent DFT calculations shed light on the importance of BH_4^- adsorption at the catalyst surface [24] (typically (111) face, Table 2), which turned out to be strong and dissociative (into BH_{ads} + 3 H_{ads}, which consumes 9 contiguous sites) on Pt, and weak and partially-dissociative on Au (into $BH_{3,ads}$ + H_{ads}, which is less site-consuming) [25,26]. Pt being able to catalyze the oxidation of co-adsorbed H_{ads} species, the DFT calculations allowed to explain its ability to achieve eight-electron oxidation of BH_4^- at potentials where H_{ads} can be ionized (above 0 V vs. RHE). On the contrary, Au requires a higher overpotential to oxidize BH_4^- [27,28] and is a poor catalyst of the HOR (3), which causes significant H_2 escape during the BOR and thus a decrease of the faradaic efficiency. Despite the fast BOR kinetics on Pt, the open-circuit potential of a Pt electrode is a mixed potential defined

Table 2
DFT-calculated adsorption energies for BOR-related adsorbates on Pt(111), Au (111), Pd(111), and Ni(111) at zero coverage limit.

Adsorbed species	Binding energy (eV)			
	Pt (111)	Au (111)	Pd (111)	Ni (111)
BH_4 *	-	-1.73[27]; -1.96[30]	-	-3.68[31]; -3.50[30]
BH+ 3 H*	-4.73[26]; -4.56[30]	-	-3.63[30]	-
BH_3 *	-1.94[26]	-0.55[27]		-2.19[31]
BH_2 *	-3.40[26]	-2.64[27]		-4.10[31]
BH*	-6.14[26]	-4.40[27]		-5.39[31]
B*	-6.50[26]	-4.43[27]		-5.75[31]
BH_3OH*		-1.08[27]		-2.77[31]
BH_2OH*	-0.06[26]	-0.06[27]		-1.27[31]
BHOH*	-3.31[26]	-2.34[27]		-3.46[31]
BOH*	-4.41[26]	-2.76[27]		-3.74[31]
$BH(OH)_2$ *	-0.17[26]	-0.05[27]		-0.49[31]
$B(OH)_2$ *	-3.09[26]	-2.20[27]		-2.36[31]
$B(OH)_3$ *	-0.16[26]			-0.22[31]
H*	-2.72[26]; -2.72[32]	-2.12[27]; -2.18[32]	-2.88[32]	-2.86[31]; -2.94[32]
OH*	-2.26[26]; -2.34[33]	-1.79[27]; -2.21[33]	-2.62[33]	-3.37[31]; -3.42[33]
H_2O*	-0.25[26]; -0.29[33]	-0.11[27]; -0.12[33]	-0.30[33]	-0.30[31]; -0.33[33]

Table 1
Comparison of various carbon-free fuels. *Calculated from the Gibbs energy of full oxidation.

Fuel	Chemical formula	Hydrogen content, mass %	State at 298 K, 1 bar	Full oxidation products	E°, V vs. RHE at 298 K	n	Energy density* ,	
							Neat MJ L^{-1}	solution (C = 1 M) kJ L^{-1}
Hydrogen	H_2	100	gas	H_2O	0[7]	2	8.4	240
Hydrazine hydrate	$N_2H_4 \bullet H_2O$	8	liquid	N_2, H_2O	-0.32[7]	4	12.3	600
Ammonia-borane	NH_3BH_3	19.6	solid	$B(OH)_4^-$, NH_4^+, H_2O	-0.39[8]	6	23.7	940
Sodium borohydride	$NaBH_4$	10.6	solid	$B(OH)_4^-$, H_2O	-0.41[7]	8	35.8	1270

by the BOR anodic current above − 0.41 V vs. RHE and the hydrogen evolution reaction (HER, which is the back reaction of the HOR, Eq.3) cathodic current below 0 V vs RHE, in such a way that a net positive current is obtained at significantly higher potential values than the thermodynamic equilibrium potential of the BOR. The DFT studies also pointed at the strong adsorption of $BH_{x,ads}$ adsorbates during the BOR (x depending on the type of the metal), which might cause poisoning of the electrode surfaces for high borohydride concentrations as confirmed experimentally [20,29].

The influence of the surface structure and the nature of adsorption sites on the BH_4^- dissociation and/or BH_x adsorption was then confirmed by Briega-Martos et al. for single-crystalline Pt electrodes [34], Pt(111) being the least active basal plane and Pt(110) the most active one (Fig. 1a). Similarly, Qin et al. showed that Pd nanocubes with (200) facets were more active than round-shaped Pd/C [35], while Olu et al. showed major effects of surface roughness for polished Pt, [36] and of crystallite size and interparticle distance (and hence loading) for glassy-carbon-supported Pt nanoparticles (Pt/GC) [37]. All these observations point to strong and surface structure-sensitive interaction between the $BH_{x,ads}$ species and the catalyst sites. It was also evidenced that the low turnover frequency of the BH_x oxidation step ultimately leads to rapid surface blocking of electrodes with low electrochemically active surface area (ECSA) and/or at high borohydride concentration (cf. Fig. 2b). It was also posited that the adsorption of such intermediates was so strong that it could lead to the reconstruction of Pd/Pt(111) surfaces [38]. In addition to the poisoning by adsorbed $BH_{x,ads}$ species, the unavoidable presence of organic impurities in solution might lead to a deactivation of the surface which manifests itself by a slow decrease of the BOR activity with time. This was notably monitored for Pt/GC by cyclic voltammetry (CV), stripping of both organic and $BH_{x,ads}$ poisons occurring in a positive scan between 0.6 and 0.8 V vs. RHE, allowing the catalyst to recover its BOR activity during the backward (negative) scan (Fig. 1b). These experiments allow one to conclude that OH_{ads} on Pt has a positive influence on the removal/stripping of $BH_{x,ads}$.

It should also be mentioned that an increase of the electrode potential beyond a certain limit (the exact value of the latter depending on the type of metal, its ECSA, and the BH_4^- concentration) leads to a drop of the BOR current (see Figs. 1b,e, 2a-c), which was attributed to the site blocking with surface oxides. Electrochemical impedance spectroscopy of Au electrodes showed that the BOR competed with Au-oxides formation at high potential, leading to surface deactivation [40]; this process is essentially similar for any noble metal surface, the onset of deactivation being lower for least noble metals (Ru < Pd < Pt < Au).

Then came studies aiming to understand the BOR mechanism and the various reaction pathways. Multiple electrochemical steps and reaction intermediates are at stake in the BOR, as expected [41]. Rotating ring-disk electrode (RRDE) using a gold ring enables to detect the formation of BH_3OH^- intermediate species, since it was shown that gold is capable of catalyzing the oxidation of borane species at 0.2 V vs. RHE, while it is still inactive for borohydride oxidation at this potential. Thus rotating ring-disk electrode studies, by Krishnan et al. (Au surfaces) [42] and by Finkelstein et al. (Au and Pt surfaces) [43], illustrated that a significant amount of BH_3OH^- could be formed in the course of the BOR on Au, but not on Pt (at least in diluted BH_4^-electrolyte). Differential electrochemical mass spectrometry (DEMS) was subsequently used to detect the molecular hydrogen escape from the diffusion layer in the course of the BOR [44]. Using borodeuteride species, Jusys et al. [39] asserted that the H_2 formed below 0 V vs. RHE comes from the HER from water, and the high-potential D_2 comes from the BOR. This hydrogen generation always accompanies BOR on Au electrodes, while on Pt electrodes it only occurs in the metal-oxide region, where Pt becomes inactive for the HOR (Fig. 1) [45]. This confirms that Au, being neither active at low potential (i.e. close to 0 V vs. RHE) nor faradaic-efficient, cannot be considered a good BOR catalyst (idem for Ag) [44,46]. Finally, using Fourier-Transform infra-red spectroscopy (FTIRS), Chatenet et al. proposed the main BOR intermediates at Au [47] and Pt [48] surfaces. On Au electrodes $BH_{3,ads}$-species are formed at low potential (E = −0.16 V vs. RHE) and $BH_{2,ads}$-species at higher potential (E = 0.16 V vs. RHE), while the final product BO_2^- is formed at 0.6 V vs.

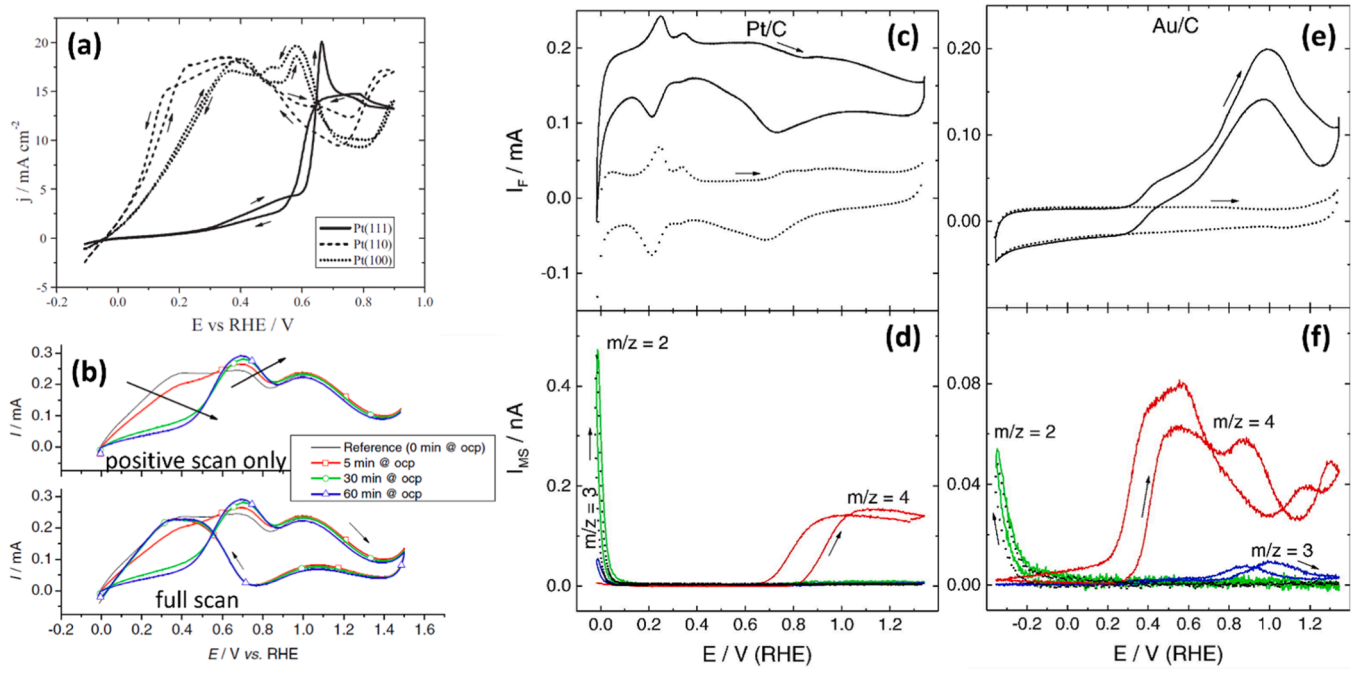

Fig. 1. (a) Cyclic voltammograms of BOR measured at Pt(hkl) basal planes in 0.1 M NaOH + 5 mM $NaBH_4$ at 50 mV s^{-1}. Reproduced from Ref. [34] with permission from Elsevier. (b) BOR voltamperograms in 1 M NaOH + 1 mM NaBHa obtained at the rotation speed of 400 rpm and a scan rate of 20 mV s^{-1} on Pt particles supported on a GC (glassy carbon) disc (Pt loading 5 μg_{Pt} cm^{-2}) after open-circuit potential hold for various durations. Reproduced from Ref. [37] with permission from Springer Nature. (c, e) Cyclic voltammograms of BOR on Pt/C and Au/C in 0.1 mM $NaBD_4$ + 0.5 M NaOH (solid curves) and 0.5 M NaOH (dotted curves) at 10 mV s^{-1}; and (d, f) corresponding online DEMS ion currents for H_2, HD and D_2 evolution. Reproduced from Ref. [39] with permission from Elsevier Ltd.

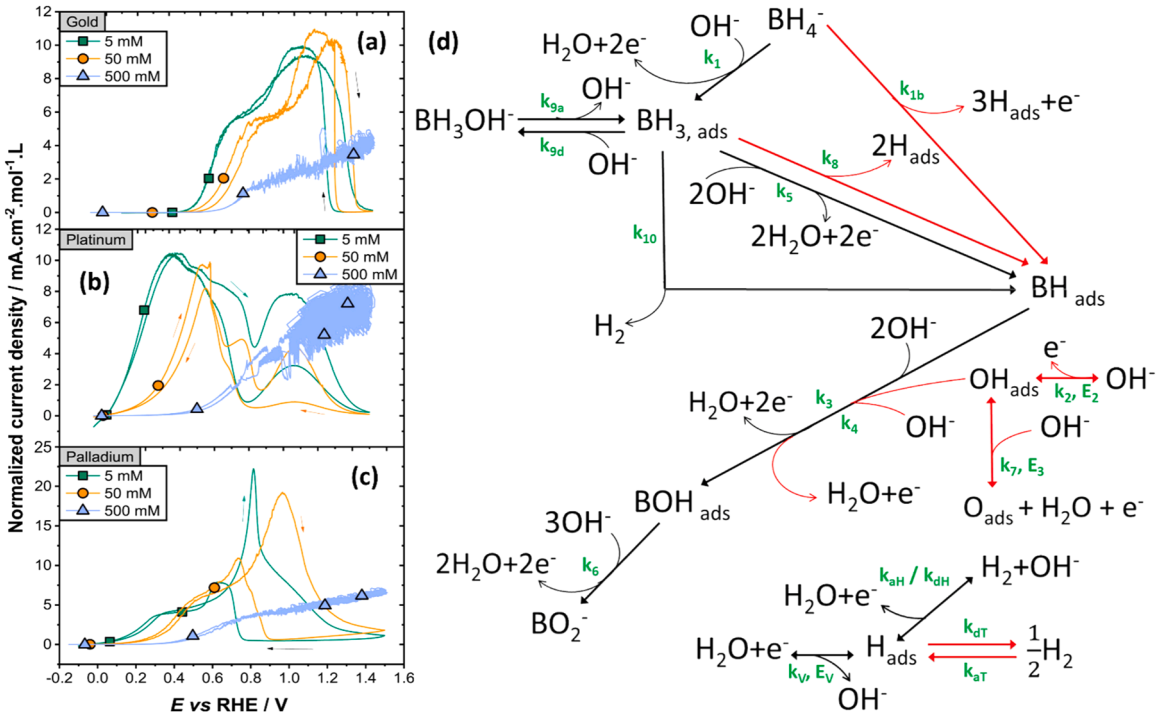

Fig. 2. Ohmic drop-corrected cyclic voltammograms of the BOR at 20 mV s^{-1} and 2500 rpm on (a) Au, (b) Pt, and (c) Pd smooth electrodes (geometric area = 0.031 cm^2) for various $NaBH_4$ concentrations in 1 M NaOH. The current density is normalized to the $NaBH_4$ concentration to illustrate the $BH_{x,ads}$ poisoning effect. Reproduced from Ref. [49] with permission from Elsevier. (d) Proposed mechanisms of the BOR on Pt and Au surfaces. Freely adapted from Ref. [50] with permission from Elsevier Ltd.

RHE [47]. Both $BH_{3,ads}$ and $BH_{2,ads}$ are likely formed on Pt in the potential interval $0.18 < E < 0.6–0.7$ V vs RHE; $BH_{3,ads}$ may be formed not only due to the BOR but also as a result of BH_4^- partial hydrolysis. The $BH_{x,ads}$ species yield BH_3OH^- upon interaction with OH^-, this species being easily electrooxidized on Pt, resulting in the final BO_2^- product in the potential interval $0.6 < E < 1.1$ V vs. RHE [48].

Armed with all these data, Olu et al. proposed the first comprehensive BOR mechanism at Pt surfaces for dilute $NaBH_4$ electrolytes (Fig. 2d) [49]. On a bare Pt surface, the BOR starts by dissociative highly Pt site-consuming adsorption of BH_4^- into $BH_{ads} + 3\ H_{ads}$; however, BH_{ads} might accumulate on the Pt surface owing to its low turnover frequency at low potential. When the potential is increased into the Pt-oxide region, hydroxyl species adsorption occurs, these OH_{ads} having a dual effect: on the one hand, they reduce the fraction of free Pt sites (negative effect); on the other hand, they react with the stable BH_{ads} intermediates in a Langmuir-Hinshelwood type electrooxidation step, thus accelerating removal of these blocking species from the Pt surface (positive effect). This mechanism was later extended to Pt and Au surfaces at larger BH_4^- concentrations, based on complete sets of experimental data [49] (Fig. 2a-c). It was concluded that while Au is never faradaic efficient (whatever the BH_4^- concentration), being incapable of valorizing H_2 that escapes (and could be detected by online DEMS), for Pt, at larger BH_4^- concentration, the poisoning from $BH_{x,ads}$ species may result in a decrease of the BOR current and lower faradaic efficiency than the one observed at lower BH_4^- concentration [50]. As a result, severely-poisoned Pt essentially behaves like Au, with a first step of partially-dissociative BH_4^- adsorption into $BH_{3,ads}$, and non-negligible H_2 and BH_3OH^- generation at low potential (Fig. 2d). The same is valid for Au, which shows a high level of H_2 escape and therefore extensively depreciated faradaic efficiency at high $NaBH_4$ concentration. Although still debated, the case of Pd is intermediate, with an apparent smaller onset potential than for Pt (especially at large $NaBH_4$ concentration, e.g. 0.5 M), but a slower low-potential kinetics and strong poisoning by $BH_{x,ads}$ species at small to medium BH_4^- concentrations (0.005 and 0.05 M) that results in lower current generation at low potential than for Pt electrodes [51]. However, some attempts were taken in order to improve the catalytic properties of Au by coupling it with various metals: AuPt alloys were found to have better charge transfer than Pt or Au-based catalysts [52], AuCo alloys also show lower charge-transfer resistance (hence faster kinetics) than Au-based catalysts [53].

What is clear from the above paragraphs, is that the BOR is a very complex reaction. Of course, not only the chemical nature of the catalyst strongly influences the shape of the current-potential curves, but also the structural properties of the catalyst layer. Freitas et al. [54] indeed demonstrated that the BOR completion is strongly related to the catalyst loading and the layer thickness. Firstly, higher catalyst loading alleviates poisoning by $BH_{x,ads}$ species: a higher number of surface sites per geometric surface area of the electrode is available at a given BH_4^- concentration. Secondly, a thicker active layer leads to a longer residence time of the reaction intermediates/byproducts (e.g. BH_3OH^- and H_2) resulting in higher conversion into final oxidation products, and hence the number of transferred electrons approaches the theoretical limit of 8 electrons per BH_4^- species. These seminal BOR studies for Pt-based electrodes were followed by Saxena et al. for dendritic Pd electrodes [55], Zhang et al. for nano-branched PdCu-based electrodes [56], and Nagle et al. for nanoporous gold electrodes [57]. While 3-electrode cell measurements are well-suited to study the reaction mechanisms and kinetics, fuel cell tests are indispensable to demonstrate the application potential of the catalytic materials and will be dealt with in Section 3.

One of the advantages of the alkaline environment of the DBFC is the possibility to use non-noble metal catalysts for the BOR. The first studies (on Ni and Cu electrodes) were attempted by Elder and Hickling in 1962 [58], who reported negligible activity of these metals below the potential of the oxygen evolution reaction (OER). Much later Suda et al. [59,60] demonstrated that Ni can catalyze the BOR at much lower potentials with the OCP (open circuit potential) being 0.15 – 0.20 V more negative than the equilibrium potential of the hydrogen electrode (3),

thus outperforming the noble-metal-based catalysts discussed above in the potential region below 0 V vs. RHE. However, along with the obvious asset of being inexpensive and abundant, a major disadvantage of Ni catalysts (spotted by Suda et al. [59,60] and later Wang et al. [61]) is their inability to catalyze the oxidation of the borohydride with a release of more than 4 electrons (against theoretical 8 e^- oxidation). The other 4 electrons are lost to the formation of two H_2 molecules per one BH_4^- species since H_2 cannot be oxidized on a metallic Ni electrode at potential close to 0 V vs. RHE.

Further studies have mainly focused on the development of Ni alloys/composites with noble metals, such as Pd [62–65], Au [66–69], Pt [15,63,68,70–74], whose BOR activity was largely determined by the second, noble metal, component. Perhaps the only exception is the study of NiRu and NiRuF catalysts with Ru content below 10 wt% by Grinberg et al. [75], in which significant and stable BOR currents were observed at potentials below 0 V vs. RHE. Among non-noble metals, the most popular additives are Co [76–78], Cu [79–83] and rare-earth metals [84–87]. One should bear in mind, however, that clear assessment of the BOR (as well as ABOR or HHOR) activity of Co-containing electrodes is complicated by the formation of multiple oxide species at the electrode surface, some of them (especially those formed below ca. 1.0 V vs. RHE) likely resulting in Co dissolution, notably at high pH [88,89]. Studies discussing the nature of the active sites in bimetallic systems are very rare and do not allow to make straightforward conclusions about the effect of the second component on the activity of Ni in the BOR. The main question is whether the second metal can catalyze the BOR at given conditions itself or rather serves to exert "electronic" and/or "geometric" effects on Ni. Although the rare-earth metals (Ce, Sm, Dy) have never been studied alone in the BOR, a decrease of the current with an increase of their content in Ni-based alloys (up to 10 at.%) likely points to their poor performance. A slight increase of the BOR currents was observed only for the Ni alloys containing 5 at.% of either of these elements, though the origin of the enhancement is not clear yet. DFT calculations suggest that Cu (111) adsorbs BH_4^- stronger than either Ag or Au [90], which agrees with electrochemical studies, showing that Cu catalyzes the BOR above ca. 0.3 V vs. RHE [82,91]. However, Cu is known to be unstable in alkaline electrolytes, forming different soluble Cu (hydr)oxides under anodic polarization. While Cu_2O in $NaBH_4$-free solutions is stable at potentials below about 0.65 V vs. RHE [92], in the presence of $NaBH_4$ it seems to be dissolved with the release of Cu^+ species (likely in the form of Cu^+ hydroxide) as reported by Vorms et al. [82]. Thus, it can be concluded that Cu only survives in the core of alloy nanoparticles, likely exerting an electronic effect on the performance of the main component (typically, Ni, Ag or Au). NiCo is the most challenging system in terms of understanding since the two metal components can adsorb BH_4^- ions and catalyze the BOR at similar conditions [90]. Some studies mention synergistic effect between Ni and Co [77,93], although its genesis is not clearly understood. In addition, amorphous Ni, Co and NiCo borides were tested in the BOR, showing promising activity and stability in a wide potential range [94,95].

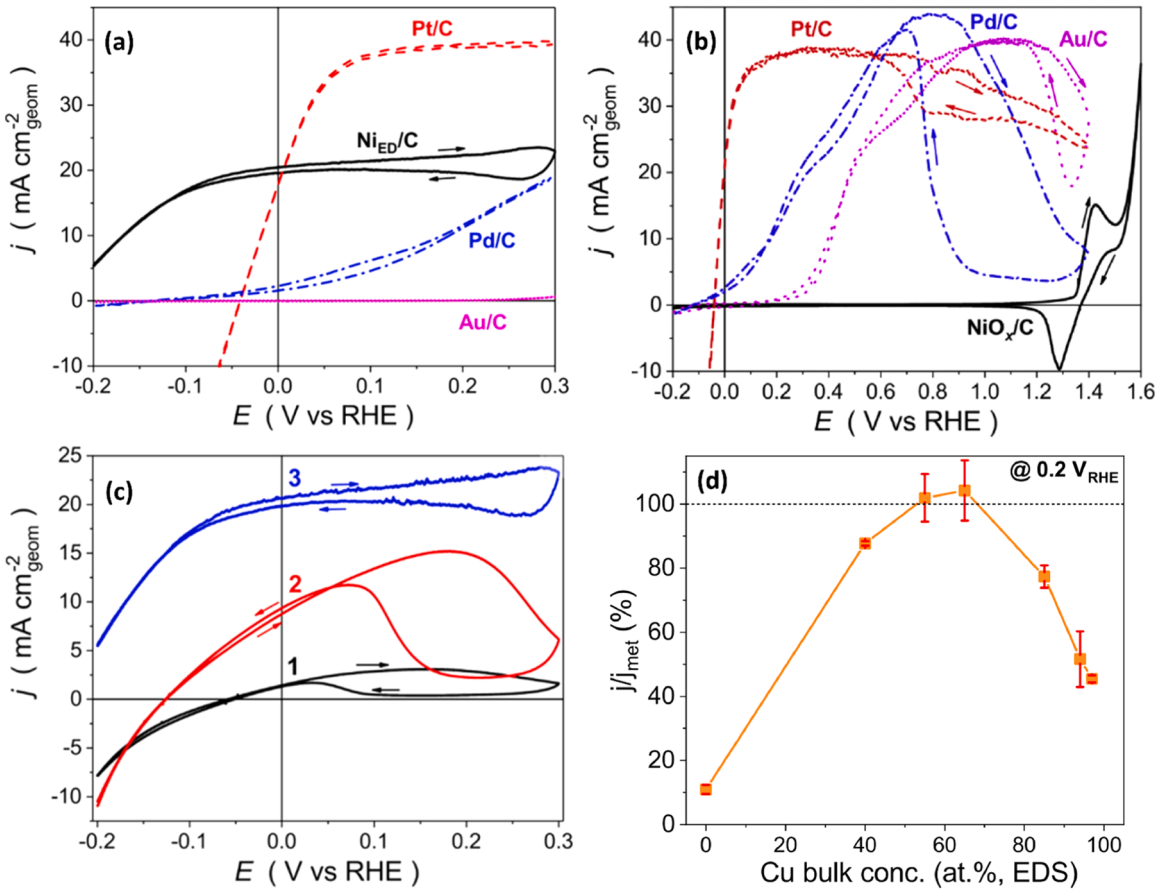

Fig. 3. (a – c) Ohmic drop-corrected (in dynamic mode) cyclic voltammograms obtained for Pt/C (dashed curve), Pd/C (dash–dotted curve), Au/C (dotted curve), and either (a) metallic Ni_{ED}/C or (b) oxidized NiO_x/C (solid curve), as well as for (c) Ni_{ED}/C electrodes at various state of their surface (1 – strongly oxidized, 2 – partially oxidized, 3 - metallic); (a, c) reproduced from Ref. [31] with permission from the American Chemical Society, (b) reproduced from Ref. [96] with permission from Elsevier Ltd.; (d) Relative BOR current (j/j_{met}) at 0.2 V vs. RHE calculated as current measured after electrode oxidation (by cycling up to 0.7 V vs RHE) divided by current measured for electrodes in the metallic state (cycled without exceeding the potential limit of 0.3 V vs. RHE) as a function of the bulk Cu concentration in the NiCu samples; reproduced from Ref. [82] with permission from Elsevier Ltd. Conditions (a – d): N_2-saturated 1.0 M NaOH + 5 mM $NaBH_4$ at v = 20 mV s^{-1} and ω = 1600 rpm.

The difficulties with the identification of the active sites for the BOR in non-noble-based catalysts largely originate from the poor control of the surface state of the catalysts in early publications. The picture recently changed, when Oshchepkov et al. [31] clearly demonstrated that only metallic Ni can be very active in the low potential region (below 0 V vs. RHE, Fig. 3a). Even slight oxidation of its surface results in a significant decrease of the BOR currents, while fully oxidized NiO_x catalysts can only oxidize borohydride in the high potential interval

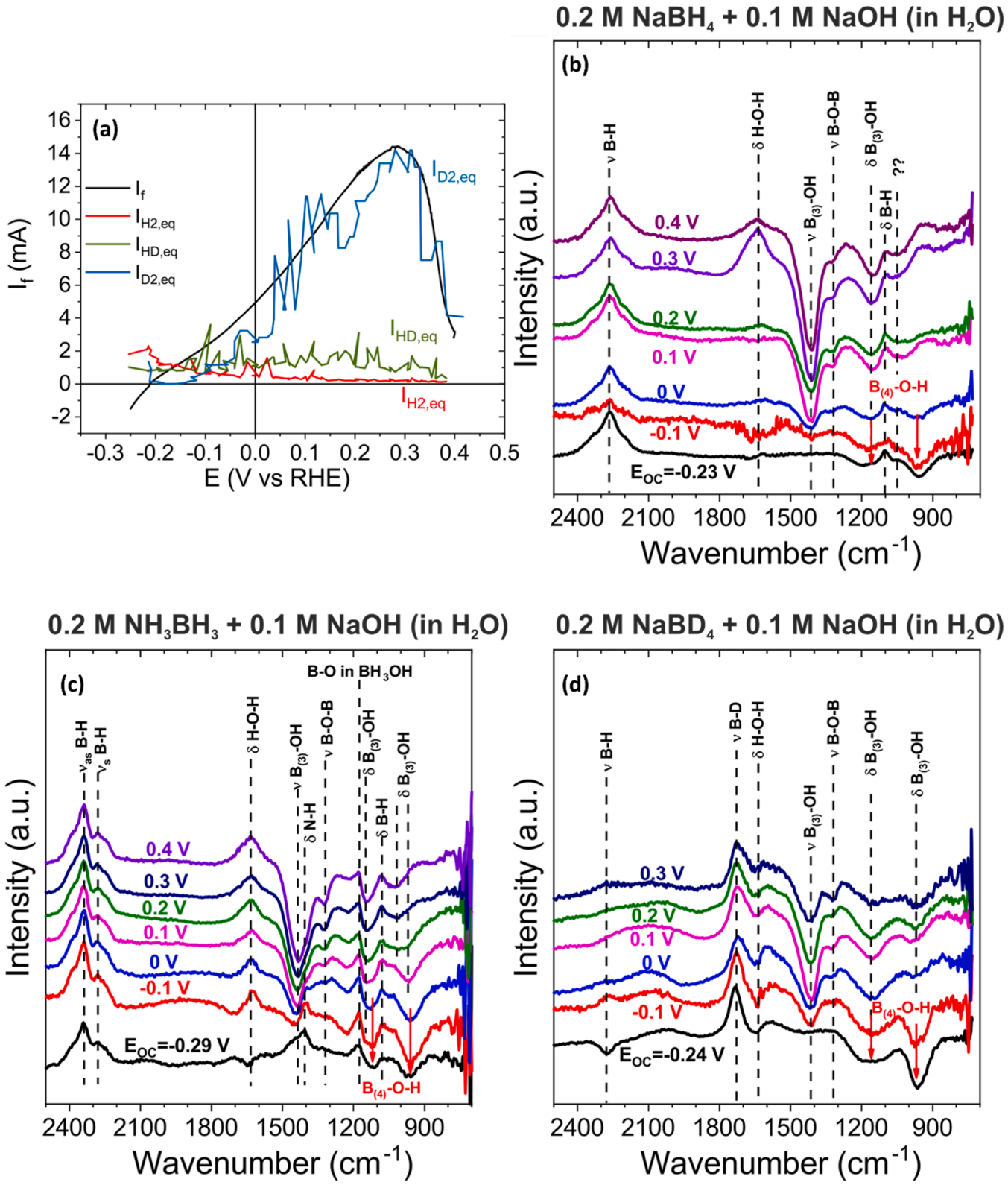

Fig. 4. (a) Online DEMS measurements of an etched Ni felt in Ar-saturated 1 M NaOH + 50 mM $NaBD_4$, $\nu = 10$ mV s^{-1}. In situ FTIR spectra of a Ni disk in (b) 0.2 M $NaBH_4$ + 0.1 M NaOH, (c) 0.2 M BH_3NH_3 + 0.1 M NaOH, (d) 0.2 M $NaBD_4$ + 0.1 M NaOD, at different electrode potentials as specified in the plots. Reproduced from Ref. [98] with permission from Elsevier Ltd.

(that is above $Ni(OH)_2$/NiOOH redox transition) (Fig. 3b). This finding allowed to reconcile the inconsistencies reported in the early literature regarding the electrocatalytic activities of Ni-based materials in the BOR. Indeed, low activity and high OCP were observed when the Ni surface was substantially oxidized, either during the preparation of the catalysts (by passivation in air) or their electrochemical evaluation (by cycling in a wide potential range, resulting in the formation of metastable β-$Ni(OH)_2$) [67,97] (Fig. 3b,c).

On the contrary, when the authors were able to keep Ni surface from being oxidized, significant BOR currents were observed already below 0 V vs. RHE [86,99,100]. Among other reasons, this noticeable BOR activity on metallic Ni electrode arises owing to the sluggish HER kinetics, the suppression of the competing HER enabling significant net BOR current at low (below 0 V vs. RHE) potentials and a negative shift of the OCP [31]. However, the low activity of metallic Ni in the HOR also results in a loss of electrons (as spotted above) due to its inability to valorize evolved hydrogen (through its oxidation), as evidenced by online DEMS (Fig. 4a) [98].

DFT simulations on Ni(111) surface predicted non-dissociative adsorption of BH_4^-, elongation of the B-H bond in an adsorbed $BH_{4,ads}$ likely facilitating the B-H bond breaking in either a purely chemical or in a potential-activated step [101]. This is in line with *in situ* FTIRS studies that show the formation of $B(OH)_4^-$ already at the OCP (Fig. 4b). Note that the changes in the spectra above 0 V vs. RHE are due to the conversion of $B(OH)_4^-$ to $B(OH)_3$ (rather than the formation of another compound/intermediate species), this chemical conversion being induced by acidification of local pH in a thin layer upon the FTIRS measurements in external reflection configuration, as evidenced by the isotope substitution measurements (Fig. 4d) and spectra of reference compounds (see Ref. [98] for more detail).

One notes in passing that alloying of Ni with other elements not only affects its electronic properties but also might help to stabilize the desired state of the surface. Oshchepkov et al. [102], while studying NiCu alloys, with the help of *ex situ* X-ray photoelectron spectroscopy (XPS) found a correlation between the Cu percentage in the Ni-based catalysts and fraction of the metallic Ni^0 phase. Armed with this information, Vorms et al. [82] investigated $Ni_xCu_{(1-x)}$ catalysts in the BOR and found that Ni-based catalysts containing Cu are more resistant to irreversible electrochemical oxidation and hence more active than pure Ni catalysts after their exposure to E = 0.7 V vs. RHE (Fig. 3d). A similar effect was observed for Ni@NiP electrocatalysts, in which an amorphous NiP shell inhibits the passivation of metallic Ni core, while also increasing the BOR activity thanks to the depreciation of the HER currents [103]. Although, to the best of the authors' knowledge, detailed studies of the effect of surface passivation of Co-based materials on their BOR performance have never been performed, it can be expected that the surface state should play an important role also in this case.

2.2. Ammonia-borane oxidation reaction (ABOR)

Studies of the oxidation of borane (BH_3) species were initiated in the field of electroplating, borane compounds being known as strong reducers. Early studies revealed the formation of hydroxyborane (BH_3OH^-) as reactive species both in ammonia-borane (AB) and dimethylamine-borane (DMAB) [101] with the final product being similar to the BOR.

$$NH_3BH_3 + 7\ OH^- \rightarrow B(OH)_4^- + 6\ e^- + 3\ H_2O + NH_3 \quad (4)$$

On Au, the oxidation of AB and DMAB bears strong similarities, except for the more deleterious poisoning effect of the DMA fragment compared to the ammonia one (both cannot be oxidized at low potentials) [104]. Pd/C was found more efficient for the direct borane oxidation, while Pt/C led to decomposition of the fuel and valorization of the H_{ads} and H_2 generated (but only above 0 V vs. RHE, while Pd/C is ABOR-active below this potential). Also, the non-borane fragment had a different fate, hydrazine being evidently more efficiently valorized at these surfaces than ammonia and DMA (see next section, relative to the hydrazine hydrate oxidation reaction). Finally, Pylypko et al. evaluated the oxidation of more complex boranes (NaB_3H_8 and $Na_2B_{12}H_{12}$), that are more suitable for safe storage, but more complex and slower to oxidize than simpler boranes, at least on Pt, Au and Pd surfaces [105,106].

Mechanistic studies of the borane oxidation reaction were however scarcer than for the BOR, and mostly concerned Au surfaces. The adsorption of DMAB on gold surfaces as a function of the potential was investigated by cyclic voltammetry and electrochemical quartz-crystal microbalance [107]. Interestingly, two abrupt mass increases attributed to two adsorbed reactive intermediate species could be evidenced. Homma investigated the mechanism of BH_3OH^- hydrolysis on Cu and Pd clusters by DFT [108] and showed that the reaction (i) is strongly sensitive to the nature of the metal surface, and (ii) proceeds via elementary steps, where OH^- complexation of the boron favors the removal of H radical to eventually form $B(OH)_4^-$. Plana et al. studied DMABOR at polycrystalline and single crystalline Au electrodes and concluded that the DMA fragment can only be oxidized at high potential (i.e. in Au-oxide region), while the borane one is more easily oxidized in a 3 + 3-electron sequence at lower potential [109,110]. From FTIRS data, they revealed that the DMAB oxidation on gold electrodes is strongly surface structure-sensitive and that the potential-dependent cleavage of the B-N bond is one of the initial steps of the oxidation process. Finally, combining DEMS, FTIRS and electrochemistry, Molina Concha et al. showed that the adsorption of the BH_3OH^- moiety on Au surfaces from a borane fuel is very different from the adsorption of a $BH_{3,ads}$ intermediate in the course of the BOR. In the former case it proceeds through the O atom, contrary to the formation of B-Au bond during the BOR; this may explain the significantly more negative 'onset' potential of borane compared to BH_4^- oxidation on Au [111].

Like for BH_4^- oxidation, numerous studies point towards the beneficial effect of nanotextured electrodes, for which larger residence time in structures containing numerous catalytic sites per BH_3OH^- species enables lower reaction onset and better reaction completion, and this was demonstrated for nanoporous Ag [112,113] and Au [114] structures. Studying different types of boranes (AB, DMAB, hydrazine-borane, HB, and hydrazine-bisborane, HBB) on Pd/C and Pt/C electrodes, Zadick et al. confirmed the residence time effects noted in the BOR, better reaction completion being reached for larger residence time of intermediates (thicker electrodes) [115].

Concerning the ABOR on non-noble metals, Filanovsky et al. studied ABOR on smooth monometallic catalysts (Fe, Ni, Co, Cu), and showed that the OCP in 1.2 M AB and 1 M NaOH lies below 0 V vs. RHE with the lowest values observed for Cu electrode [116]. By preparing a nanotextured Cu with a high surface area, the same authors were able to significantly increase the ABOR currents, outperforming the commercial Pt/C catalyst in a wide potential range. Similar to the BOR, the surface state of non-noble metal catalysts has never been controlled in the ABOR studies, which likely explains the large difference between the OCP on Cu (which can be easily reduced electrochemically), and other less 'noble' electrodes. Indeed, Zadick et al. observed a continuous decrease in the OCP (hence activity increase) of Ni_3Co/C in the ABOR upon surface reduction, with the final value being around − 0.1 V vs. RHE. [117] At the same time, Oshchepkov et al. reported that the OCP for metallic Ni disk in the presence of NH_3BH_3 is ca. 60 mV lower compared to $NaBH_4$ (E_{OC} = −0.29 and −0.23 V vs. RHE for NH_3BH_3 and $NaBH_4$, respectively), which points to faster oxidation of BH_3OH^- compared to BH_4^- ions, possibly due to differences in BH_4^- and BH_3OH^- adsorption configuration on the Ni surface (as discussed above for Au electrodes) [98]. The final product, $B(OH)_4^-$, is identical for BOR and ABOR, as ascertained by the FTIRS studies (Fig. 4c). Recently, several Ni-based porous electrodes with high surface area, including Cu-doped Ni $(PO_3)_2$ [118], $Ni_{1-x}M_xSe_2$ (M = Cu, Fe, Co) [119] and $Ni_{1-x}Cu_xO$ [81] nanowire arrays on carbon fiber paper, were reported. All of these materials showed an OCP below − 0.28 V vs. RHE in the presence of AB.

Importantly, the diffusion-limiting currents on the $Ni_{1-x}Cu_xO$ electrode were observed at $E > 0.05$ V vs. RHE with a number of released electrons around 5.8, which is close to the theoretical maximum (6). The latter is achieved thanks to the complete valorization of produced H_2 at these potentials, as confirmed by the DEMS and RRDE measurements. Note however that the complex initial structure and composition of the recently developed catalysts as well as a highly reductive atmosphere of the AB complicate the understanding of the nature of the active sites, which under steady-state conditions should comprise metallic rather than metal oxide sites.

2.3. Hydrazine hydrate oxidation reaction (HHOR)

Hydrazine is a common reducing agent, which has found vast application as a fuel because of its high energy density. The latter justifies the broad interest in studying the hydrazine hydrate oxidation reaction (HHOR, the notation reflecting the use of hydrazine in aqueous media) over the past decades, notably in alkaline media, where the rate of electrooxidation and the stability of the fuel against decomposition (see below) are higher [120].

Electrochemical HHOR theoretically involves the transfer of 4 electrons and results in the formation of N_2 and H_2O:

$$N_2H_4 + 4\ OH^- \rightarrow N_2 + 4\ H_2O + 4\ e^- \quad (5)$$

$E^\circ = -0.33$ V vs. RHE).

However, parallel to the electrochemical (desired) pathway, chemical decomposition of hydrazine may occur, resulting in either ammonia (6) or hydrogen (7), whose contribution depends on pH, hydrazine concentration (both factors can be accounted for by Eq. (8) proposed by Heitbaum & Vielstich for Pt [121]) as well as the catalyst type (for example, Co and Ni catalysts were reported to favor the decomposition through the Eq. (6) and eq. (7), respectively [122]).

$$N_2H_4 \rightarrow 4\ NH_3 + N_2 \quad (6)$$

$$N_2H_4 \rightarrow N_2 + 2\ H_2 \quad (7)$$

$$(6+y)\ N_2H_4 \rightarrow 8\ NH_3 + (y+2)\ N_2 + 2\ y\ H_2 \quad (8)$$

where $y = [OH^-]/[N_2H_4]$.

The mechanism of the hydrazine adsorption/decomposition on metals has been widely studied both at solid/liquid and solid/gas interface, thanks to the low boiling temperature of hydrazine, which differs significantly from either borohydride or ammonia-borane. Besides, non-noble metals were as widely studied for HHOR catalysis as noble ones, which allows one to simultaneously discuss the reaction mechanism for both.

In the first studies of the mechanism of the HHOR on Pt, Pavela [123] suggested that hydrazine decomposes with formation of adsorbed hydrogen atoms (H_{ads}, Eq. (9), followed by their electrochemical oxidation (10):

$$N_2H_4 = N_2 + 4\ H_{ads} \quad (9)$$

$$H_{ads} + OH^- = H_2O + e^- \quad (10)$$

At OCP, which on many metals (both noble (Rh, Ru) [124] and non-noble ones (Ni, Co)[125]) lies between the equilibrium potential of the HHOR and the HOR/HER, decomposition of hydrazine is observed and leads to the formation of N_2 and H_2 (7). Hydrazine decomposition may be considered as a sum of two electrochemical reactions: the HHOR (5) and the HER, pointing to the involvement of H_{ads} in the overall reaction mechanism [125]. This indeed has been confirmed by Korovin et al. based on the measurements of hydrogen absorbed by Pd thin membrane during the HHOR, [126] and later by Fukumoto et al. for Pt, Rh, Pd, Ni and Co [127]. Harrison and Khan have demonstrated that the HHOR current on Pt is proportional to $[OH^-]^4$ ($[OH^-]$ standing for the hydroxide ion concentration), with the fast exchange of 3 first electrons and the last electron-transfer being the rate-determining step [128]. The mechanism of the HHOR was further refined by Kodera at al. [129] at Pt, who suggested electrochemical formation of $N_2H_{2,ad}$ (11), followed by its rate-determining chemical decomposition (12) to produce H_{ads}, the latter being further ionized following Eq. (10).

$$N_2H_4 + 2OH^- = N_2H_{2,ads} + 2\ H_2O + 2e^- \quad (11)$$

$$N_2H_{2,ads} = N_2H_{ads} + H_{ads} \quad (12)$$

DEMS studies of Rosca et al. of the HHOR on Pt basal planes (Fig. 5a, b) evidenced formation of N_2 (but no NO_x species) and supported participation of adsorbed intermediates in the HHOR. The activity declines in the sequence Pt(110) > Pt(100) > Pt(111) (Fig. 5a, b) [130]. It was concluded that at low overpotentials, the HHOR on Pt(110) and Pt (111) surfaces is limited by electrochemical steps (coupled electron and proton transfer), whereas on Pt(100) a chemical step involving $N_2H_{2,ads}$ dissociation is rate-determining. A similar result was obtained for preferentially-shaped Pd nanocrystals [131]. However, the nature of the stable adsorbed intermediates (responsible for the rate-determining step) is likely to depend on the nature of the catalyst as well as the operating conditions (concentration of N_2H_4, pH, temperature, etc.), so that Eqs. (11) and (12) can be replaced by more general Eqs. (13) and (14) suggested by Korovin et al. [126]. Besides, H_{ads} can lead to the formation of some H_2, which was indeed observed by Takehara et al. [132] during the HHOR on Pt, Pd and Ni. Importantly, isotopic studies ($^{14}N_2H_4$ and $^{15}N_2H_4$) performed on Pt, Ni and Pd point to the intramolecular formation of N_2, thus suggesting the absence of N-N bond splitting during the HHOR [133–135].

$$N_2H_{4,ads} + (4\text{-}x)\ OH^- = N_2H_{x,ads} + (4\text{-}x)\ H_2O + (4\text{-}x)\ e^- \quad (13)$$

$$N_2H_{x,ads} = N_2 + x\ H_{ads} \quad (14)$$

To better understand the hydrazine decomposition/oxidation reactions, Alberas et al. [136] appliedXPS to detect surface adsorbates on Pt(111) after surface exposure to hydrazine at 55 K, resulting in multilayer adsorption of N_2H_4. When the temperature was increased to 200 K, the N 1s peak splitting into two components was observed (Fig. 5e) and rationalized by the formation of N_2H_x ($x \leq 4$) bonded to the Pt surface through either one (*anti*- and *gauche*-conformation, Figs. 5f, 5g) or two (*cis*-conformation, Fig. 5h) N atoms. The higher intensity of the low binding energy N 1s peak (i.e. stronger bonded N atoms) agrees with DFT calculations, suggesting the *cis*-conformation as the most stable configuration of adsorbed N_2H_4 on Pt(111) [137]. Similar solid/gas studies (using electron energy loss spectroscopy) on Ni(111) [138] and Ir/Ni[139] revealed the formation of NH_{ads} and $NH_{2,ads}$ intermediates above 285 K, while DFT calculations showed that N_2H_3 and N_2H_2 adsorbates are rather stable on the Ni(111) surface [140], preferentially present in *anti*-conformation [141].

Along with H_{ads}, and $N_2H_{x,ads}$, oxygen-containing adsorbates (O_{ads} and/or OH_{ads}) also play an important role in the HHOR. Indeed, Finkelstein et al., who evaluated many transition metal surfaces for the alkaline HHOR using a rotating disk electrode (Table 3), found that depending on the metal at stake, the OH_{ads} and O_{ads} species could either poison or accelerate the HHOR [124], in line with the ubiquitous role of OH_{ads} in the BOR mentioned above. Indeed, similar to the BOR, the reactivity of noble metals in the HHOR decreases in the order Pt > Pd > Au (Fig. 6a) with Rh, Ru and Ir showing even lower OCP (Table 3). The HHOR on Ni takes place at low (metallic surface) and high (oxidized surface) potentials (Fig. 6b), suggesting a significant influence of the surface state on the reaction kinetics [142]. The negative impact of the Ni surface passivation/competitive OH adsorption on the HHOR has also been seen by Burke et al.[143] and Jeon et al. [144]. As for the activity of Co-based electrodes, one cannot exclude that high overall currents may (partially) result from the Co anode oxidation/dissolution (see also Section 2.1), which explains the significant difference in the performance of Co and Ni catalysts in the HHOR [124,145,146]. The latter,

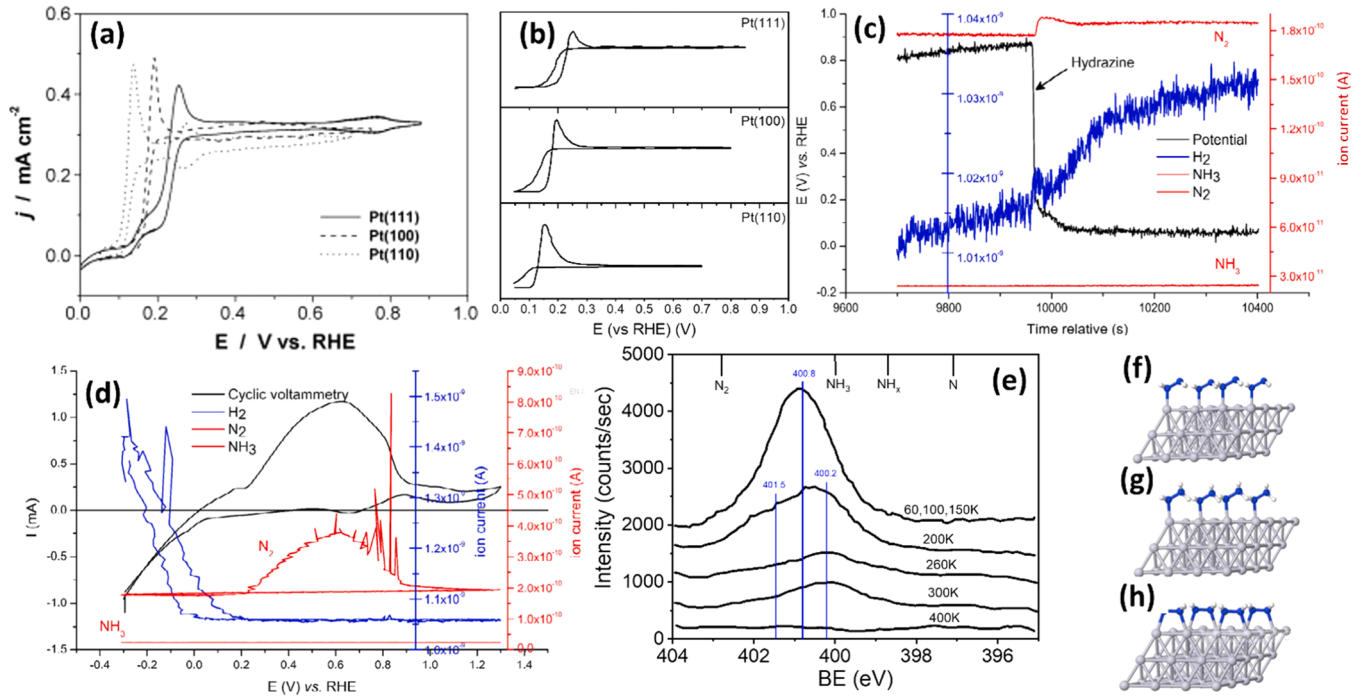

Fig. 5. (a) Cyclic voltammograms of the HHOR at Pt(hkl) surfaces in 0.1 M NaOH + 0.82 mM N_2H_4 at 20 mV s^{-1}, and (b) corresponding on-line DEMS measurements of the m/z = 28. Reproduced from Ref. [130] with permission from Elsevier Ltd. DEMS studies of the HHOR on Pd showing (c) a slight chemical decomposition of hydrazine into N_2 and H_2 (but no NH_3) at OCP and (d) an absence of H_2 in the potential interval of the HHOR. Cyclic voltammogram recorded at 20 mV s^{-1} in 0.1 M NaOH + 5 mM N_2H_4. Reproduced from Ref. [115] with permission from the American Chemical Society. (e) N 1s XP spectra of N_2H_4 adsorbed on clean Pt(111) at 55 K and subsequently heated briefly to the indicated temperature (re-cooled to take XP spectrum). Reproduced from Ref. [136] with permission from Elsevier Ltd.; DFT calculated stable configurations of N_2H_4 on Pt(111) in (f) anti-, (g) gauche- and (h) cis-conformation. Reproduced from Ref. [137] with permission from Elsevier Ltd.

Table 3
Selected characteristics of the HHOR on polycrystalline metal electrodes obtained based on the rotating disc electrode measurements in 5 mM N_2H_4 in 1 M NaOH at 500 rpm.

Metal	*n* of electrons	1 M NaOH	
		E_{OCP} (V vs. RHE)	$E_{1/2}$* at 500 rpm (V vs. RHE)
Pt	4	0.105	0.190
Pd	4	0.175	0.240
Rh	4	-0.010	0.060
Ru	3, 2.5, 1.5	-0.030	0.010
Ir	3	0.090	0.120
Au	4	0.530	0.530
Ag	4	0.510	0.715
Ni	3, 2.5, 1.5	0.020	0.160
Co	1.7	-0.052	0.160

* $E_{1/2}$ stands for the half-wave potential.
Source:Reproduced from Finkelstein et al. [124].

though with some differences, may also apply to the Cu catalysts [145, 147].

By employing the OH-donor behavior of the NiO_x moieties that facilitate the $H_{ads\ conversion}$ into H_2O, De Oliveira et al. prepared NiO_x-covered Pt/C with higher HHOR activity and selectivity than Pt/C, [148] hereby confirming the results of Ye et al. with PdNi-based catalysts [149]. Zadick et al. also showed that Pd was a very efficient HHOR catalyst, active at rather low potentials [115], the reaction being selective towards the desired N_2 product, with very little H_2 and NH_3 byproduct formation at potentials above the OCP (Figs. 5c, 5d). Many attempts were made to improve Ni activity by alloying with Cu [150], Co [151,152], Mn [153], Fe [153], Zn [153], and other metals. Importantly, Feng et al. [154] proposed that the positive effect of Zn likely originates from its ability to prevent Ni oxidation. Meanwhile, according to Zhang et al. [155], Fe alloyed with Ni inhibits hydrazine decomposition. On the contrary, NiIr [156] and NiPt [157,158] catalysts as well as CuPt [159] were found to be more active towards hydrazine decomposition than Ni catalysts, which makes them less promising for the HHOR.

To conclude, the alkaline HHOR is one of the reactions where noble metal-free catalysts are very competitive and even outperforming noble metals (similar to what was shown in Section 2.1 for the BOR) [145], which explains why many recent studies have been performed on 3d-transition metals.

3. Fuel cells

3.1. Direct Borohydride Fuel Cells (DBFC)

Discovered 2 decades ago [9], DBFCs have been under extensive focus in the 2000s and 2010s. Most of the studies were simply based on a trial-and-error approach, and thus convey little fundamental interest. Nevertheless, the fast BOR enables significant anode performance, and, if the membrane and cathode are not limiting, remarkable cell performance can be achieved with a liquid fuel that is far easier to store than the H_2 gas. This has stimulated industrial developments (Medis technologies/More Energy Ltd, MERIT Ltd) as well as intense research for small portable applications, and for unmanned vehicles for aerial and submarine purposes [160,161]. There are many different possible configurations to build a DBFC, with a cation-exchange or an anion-exchange membrane (all of these configurations have been extensively reviewed [96,162,163], Figure 7a), a bipolar membrane [164–166], a simple separator [167], or even without separation (and fuel/oxidant tolerant cathodes/anodes), which has been demonstrated by the group of Gyenge [168,169] (Figure 7b) and of Abruna in a microfluidic approach [170].

The nature of the oxidant can be varied from O_2 or air, H_2O_2 to even other strong oxidants like Ce^{3+}, VO_2^+, ClO^- or MnO_4 based catholytes

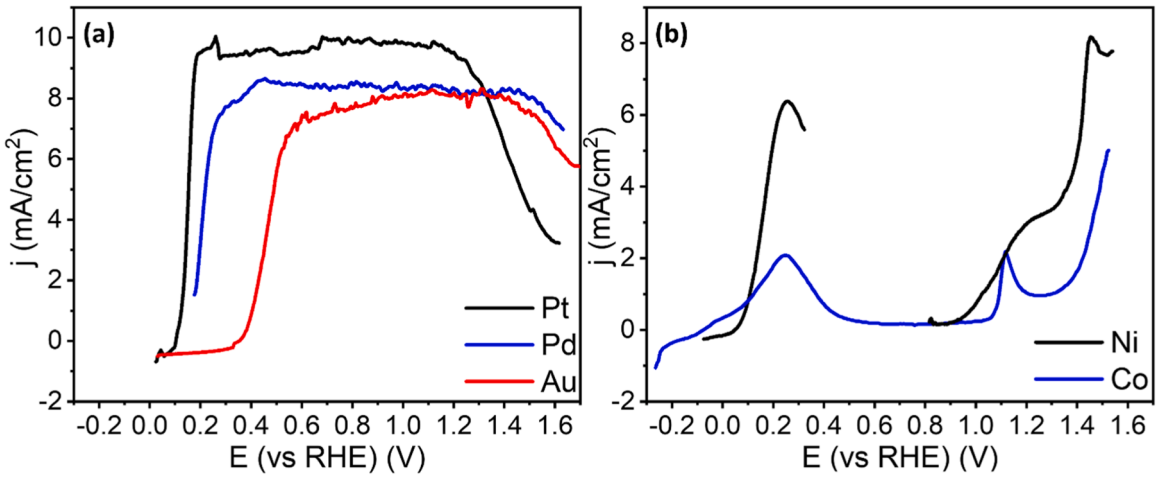

Fig. 6. Cyclic voltammograms (only forward scans are shown) recorded in 1 M NaOH + 5 mM N_2H_4, at 20 mVs^{-1}, and 500 rpm for (a) Pt, Pd, Au and (b) Ni and Co. Reproduced from Ref. [124] with permission from Elsevier Ltd.

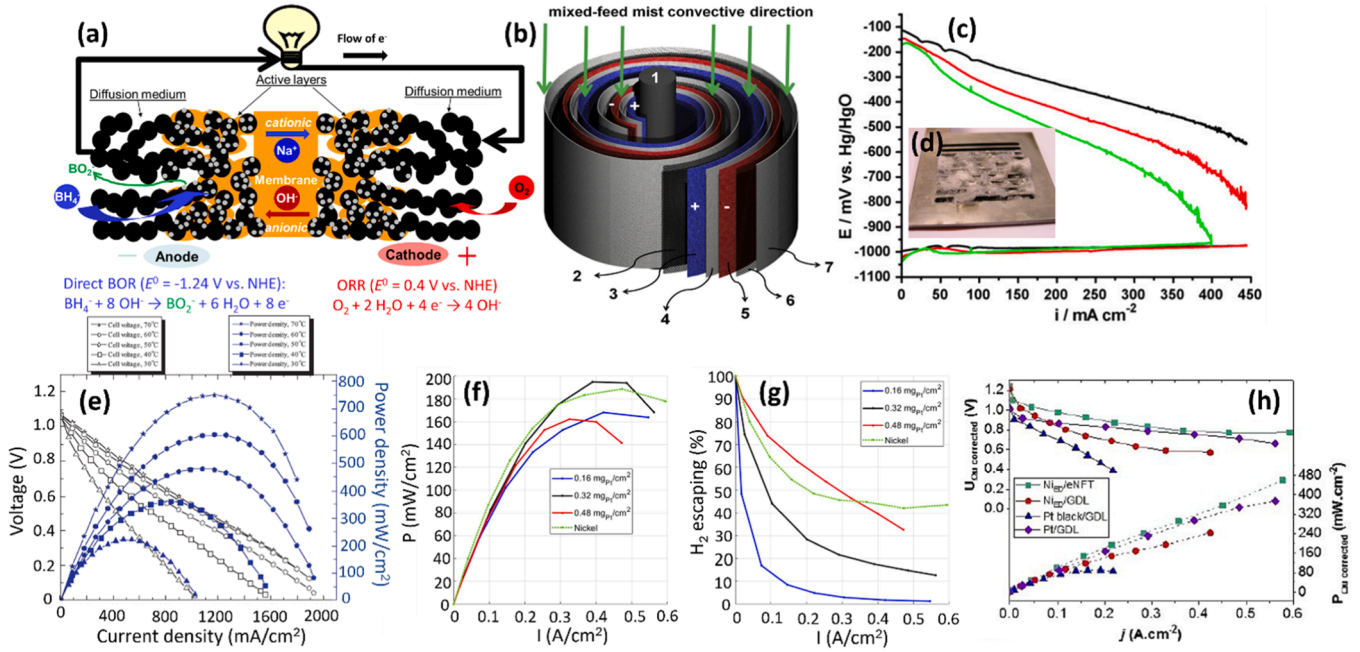

Figure 7. (a) Schematics of a membrane-based DBFC (with O_2 as an oxidant) and related anode and cathode reactions and (b) of a so-called Swiss-roll membraneless DBFC. (b) is reproduced from Ref. [169] with permission of Elsevier Ltd.; the reader should refer to this reference for the detailed explanation of the scheme (b); (c) Non-limiting anode and limiting cathode potentials measured in an operating DBFC. The inset (d) is a photograph of the air cathode current collector after tests, showing precipitates of NaOH, $NaBO_2$ and $NaBH_4$. Reproduced from Ref. [171] with permission from Elsevier Ltd. (e) Current-voltage and power density plots for DBFC employing a Chitosan anion-exchange membrane and a (Ni + Pd/C)/Ni foam anode. Reproduced from [172] with permission from Elsevier Ltd. (f) Electrical power output for three platinum charges and the nickel electrode described in Ref. [191]. (g) Corresponding output hydrogen flow rates as a function of the current density (so-called hydrogen escape, expressed in % of the generated current density). Reproduced from Ref. [191] with permission from Elsevier Ltd. (h) DBFC performance of the Ni_{ED}/NFT electrode compared to those of Ni_{ED}/GDL and Pt black/GDL and Pt/GDL (60°C, 0.5 M $NaBH_4$ + 4 M NaOH electrolyte flow rate 50 mL min^{-1}). Reproduced from Ref. [174] with permission from Wiley-VCH Verlag.

[170,175]. In many DBFC literature studies, it is not always clear whether the limitation of the DBFC comes from the anode (in rare occasions, the cathode is known to be limiting [63,171,176], as clearly seen in Figure 7c), although the anode is often the main object of the study; this is a real bias in the level of confidence one can have in the studies. In any case, the processes at stake in a DBFC are very complex, and there are many sources of limitation. Among others, one can cite the hydrogen evolution and escape (related to the possible BOR below the RHE potential and/or to the heterogeneous hydrolysis of BH_4^-), the BH_4^- cross-over (possible with a cation-exchange membrane and very likely with an anion-exchange membrane) [177–179] and related tolerance of the cathode catalyst to strong reducers (the choice of the cathode catalyst is therefore pivotal to the cell performance [163,180–182]), the cathode deactivation by NaOH (especially for DBFC based on a cation-exchange membrane [183]), carbonates and $NaBO_2$ product [171] (Figure 7d). The fuel feed composition (e.g. ratio between OH^- and BH_4^- concentrations), the flow and temperature, are also determining the overall anode (and the cell) performance [184]. As such, the engineering of the DBFC and notably of its anode is pivotal for reaching acceptable performance, not to mention the cell and materials durability, which is far from granted in strong alkaline conditions [185–188]. The following paragraphs will emphasize these aspects.

The DBFC anode catalysts have been the subject of numerous studies in the literature, and some reviews are worth reading [189,190]. Already diverse on the BOR (see Section 2), the literature of DBFC anode catalysts is also extremely broad. Many studies focus on Au-based catalysts, but it is no surprise that such anodes have poor performance, Au being intrinsically not a good BOR catalyst (see above). On the contrary, DBFCs usually perform well when they employ anode catalysts based on (a combination of) Pt, Pd and Ni. For example, the best-ever performances (to the authors' knowledge) obtained in DBFCs (810 and 890 mW cm^{-2}, respectively, Figure 7e) were reached with (i) a (Ni + Pd/C) anode catalyst (5 $mg_{catalyst}$ cm^{-2}) supported on a Ni foam (open structure), in a system using a Chitosan anion-exchange membrane operated at 70 °C, a Pt/C cathode catalyst fed with pure O_2, a 5 wt.% $NaBH_4$ in 10 wt.% NaOH anolyte fed at very high stoichiometries (> 40 at j_{max} for BH_4^-, > 43 at j_{max} for O_2) [172] and (ii) a Pd/C/Ni foam anode catalyst at the interface with a bipolar membrane [173]. In that second case, the engineering of the cell was particularly tailored. Section 2 made this predictable, as both Ni and Pd show very low BOR onset potential values and decent BOR kinetics, even at large $NaBH_4$ concentrations (the usual situation in a DBFC). Pure platinum and nickel anodes are also capable of leading to rather high cell performance (Figure 7f), though the hydrogen escape can be an issue, especially at high cell voltage for Pt and at any current for Ni (Figure 7g).

What is evident in Figure 7(e-h) as in many studies of the literature, is that the engineering of the anode significantly affects the overall cell output. Firstly, adapting the anode loading to the anolyte composition enables better management of the H_2 escape without compromising the power density (Figure 7 f, 7 g) [191]. Indeed, the mass-transport to/from the anode is very complex, as it involves BH_4^- diffusion/convection, and even migration in the liquid phase, H_2 bubbles may form on the electrode surface and block access to the active sites [192], and boron-oxides (the final product of the BOR) may precipitate in the anode porous structure [171]. For these reasons, the ways to enhance mass-transport are under intense focus, and strategies of using open structures (meshes, foams) [179,193], turbulence promoters [194], or deliberately cracked active layers [186] enable to reach high performance. The pattern of the flow-field channels to the anode also enables optimization of the liquid/gas flows to/from the anode, hence mitigating hydrolysis and better managing H_2 escape [62,173,184]. In addition, graded anodes based on Pd/C and Pt/C led to better performance than corresponding mixed anodes with (Pd/C + Pt/C) and individual component anodes [195].

The latest developments of DBFC combined many of these strategies (Figure 7 h); metallic Section 2 electrodeposited nickel (Ni_{ED}) anodes on 3D-structured nickel felts (NFT) outperform Ni_{ED}-based and Pt-based anodes supported on conventional carbon-based gas-diffusion layer (GDL) [174]. The improved performance originates from the Ni-metal surface (very active for the BOR, rather inactive for the HER, see Section 2), high electroactive area obtained thanks to Ni-metal electrodeposition, and the very open architecture of the anode (open porosity), that enables appropriate removal of H_2 bubbles and anolyte flow. Such anodes were also successfully employed in H_2O_2 DBFC bearing a bipolar membrane [190].

3.2. Borane fuel cells

Direct borane fuel cells (borane originating from AB, DMAB, or HB) have been much less studied than their borohydride counterpart. Only a few studies can be mentioned, like that of Auxilia et al. that used a mesoporous Cu anode to oxidize AB in a DABFC [196] and Zhang et al. that characterized a DABFC using Pt/C electrodes and a cation-exchange membrane (poor performance being obtained: 14 mW cm^{-2}) [8] and a DHBFC operated with a Co-based anode in interface with a cation-exchange membrane [197]; in that latter case, the Co anode enabled lower HBOR onset than Pt/C and Ni/C anodes, Pt/C enabling larger power density but lower efficiency.

In the end, the only study (to the authors' knowledge) that led to an appreciable performance with a borane fuel was the one of Olu et al. [186]. The results show how using Pt/C anodes and $NaBH_4$ fuel leads to (slightly) better performance than Pd/C anodes and an AB fuel (Fig. 8).

3.3. Direct hydrazine hydrate fuel cells (DHHFC)

Firstly tested in the 1970s [198], alkaline direct hydrazine hydrate fuel cells (DHHFC) have witnessed some success in the last two decades, mainly owing to the effort of Daihatsu to use such systems for powering vehicles (small cars and then small trucks) [199]. Indeed, hydrazine hydrate can be transported in pipes like gasoline, which would make the refueling of the vehicle rather convenient [200]. Cation and anion-exchange membranes were tested, the latter ones enabling better performance owing to a smaller fuel crossover [201]. The same conclusion was made in Ref. [202]; moreover, it was found that when using a mixed $NaBH_4$-N_2H_4 fuel and a cation-exchange membrane as the electrolyte, the concentration of N_2H_4 does not affect the open circuit voltage (OCV) of the cell but improves the power density, while when using an anion exchange membrane (AEM), the increase of the N_2H_4 concentration improves both the cell OCV and the power density. The latter was explained by a possible formation of $N_2H_5^+$ BH_4^- complex, which would reduce the crossover of BH_4^- through the AEM.

As in the case of DBFCs, great attention is paid to the anode catalysts of the DHHFC and very little to the cathode catalysts and the processes occurring in the cathode compartment; this is of course not ideal to reach a full understanding of the results. Many anode catalysts had been evaluated, from platinum-group metals [203] to non-noble ones [204], and for evident commercialization purposes, the latter were privileged [205]. In particular, catalysts based on nickel have real assets [204], having a smaller HHOR onset than platinum based-catalysts [145] and a smaller rate of hydrazine decomposition (hydrolysis) than cobalt-based catalysts, hence minimizing the rate of (undesired) NH_3 production [204]. Nickel can be combined with Co [206], Zn [207] or La [153,208], the second element stabilizing the oxidation state of the Ni surface under operation. As a result, using a NiZn anode catalyst in a DHHFC may be seen as a reasonable compromise between large power density and low NH_3 formation (Figs. 9) [207]. There have also been attempts to improve Ni catalytic performance by introducing noble metals: Hosseini et al. [209] concluded that among NiPt, NiPd and NiRu core-shell nanoparticles, Pd-based ones show the best activity, durability and power density in the fuel cell tests. Additional works have been dedicated to the improvement of the noble metal performance by alloying with non-noble metals. Crisafulli et al. [210] found that alloying Pd with Cu allows to greatly improve the behavior of the former as an anode catalyst in the DHHFC, which was, inter alia, attributed to OH_{ads}/O_{ads} on Cu facilitating fuel oxidation. Adding Ni to Pd-based catalysts was found to increase their catalytic activity and durability [211].

Lu et al. [212] drew attention to the negative effect of the gas bubbles formed during the HHOR, which accumulate on the catalyst surface and hinder the fuel mass transport to the catalyst surface, therefore reducing the HHOR performance. Moreover, gas bubbles create pressure that causes degradation of the catalyst. Lu et al. suggested the nanoporous structure of a Cu catalyst allowing to reduce adhesion forces and hence facilitate the release of nitrogen bubbles. The nanostructured Cu film was tested in a DHHFC and showed two times higher power density than a commercial Pt catalyst. One could also mention super aerophobic catalysts based on graphene and reported by Akbar et al. [213], however, the onset potential lies at $E > 0.6$ V vs. RHE, too high to be really interesting for energy harvesting.

The effect of the pH on the DHHFC performance was studied by Yin et al. [214]. Using ZrNi alloy as the anode catalyst and carbon-supported Pt as the cathode catalyst for the H_2O_2 reduction reaction, fuel cell tests showed that adding NaOH to the aqueous electrolyte improves DHHFC performance with either a cation- or an anion-exchange membrane. Furthermore, it was concluded that the OH^- concentration influences the

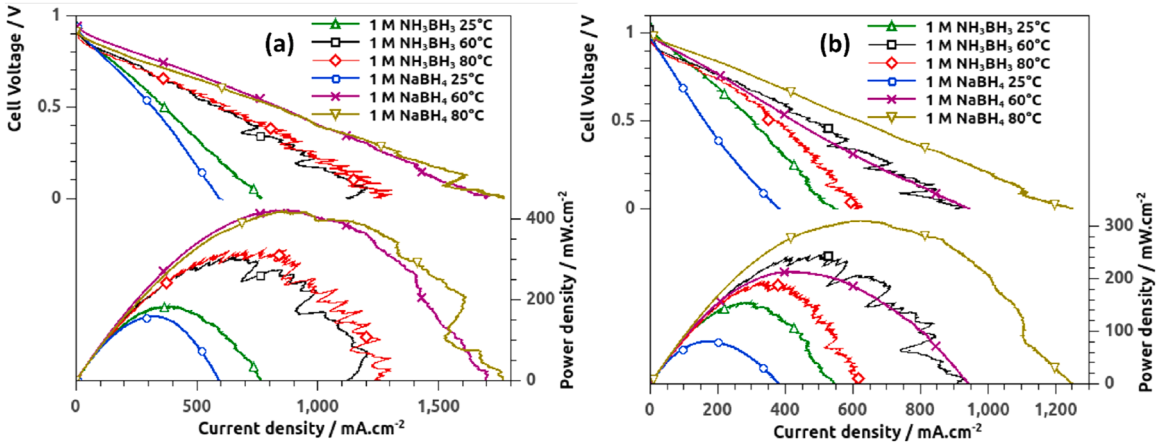

Fig. 8. Comparison of the performance of DABFC and DBFC using (A) Pt/C and (B) Pd/C anodes (0.5 mg of Pt or Pd per cm^2) fed by 5 M NaOH with either 1 M $NaBH_4$ or 1 M AB, commercial Pt/C on Toray paper as cathode catalyst fed by pure oxygen and Nafion® NRE-212 cationic membrane. Reproduced from Ref. [186] with permission from Elsevier Ltd.

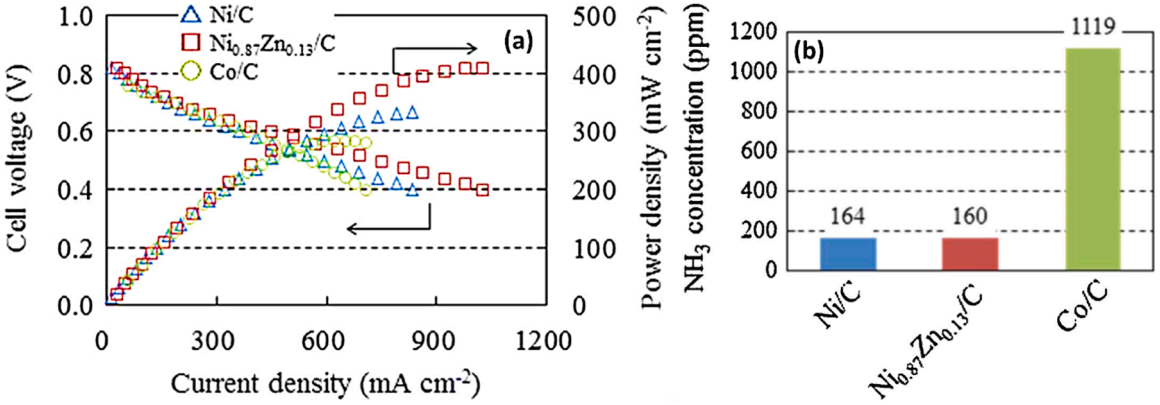

Fig. 9. (a) Performance of DHHFC using various anode catalysts and (b) corresponding NH_3 detection in the fuel outlet at open circuit. Reproduced from [207] with permission from Elsevier Ltd.

cathode overpotential stronger than the anode one. The OH^- concentration effect on the N_2H_4/O_2 fuel cell performance was discussed by Asazawa et al. [204]. It was found that the power density improves with increasing KOH concentration until 1 M (attributed to an improved conductivity of the electrolyte), but goes down at the KOH concentration of 3 M (which was attributed to the negative impact of pH on the oxygen reduction reaction at the cathode). Along with the KOH, the effect of the N_2H_4 concentration was studied and the maximum cell performance was observed with a 4 M N_2H_4. The observed decrease of the power density at higher concentrations may point to an eventual poisoning of the Ni-based catalyst or insufficient OH^-/ N_2H_4 ratio.

Regarding oxidants other than O_2, the influence of the H_2O_2 concentration in the cathode compartment on the DHHFC performance was investigated by Hosseini et al. [209]: the OCV increased with increasing the H_2O_2 concentration from 0.5 M to 2 M, following the Nernst equation; however, the power density decreased with an increasing H_2O_2 concentration, due to the H_2O_2 decomposition. Besides H_2O_2, other interesting oxidants were tested at the cathode compartment in DHHFCs: Kim et al. [215] suggested feeding CO_2 to the cathode compartment, therefore the DHHFC would produce not only electricity but also valuable carbon-containing products. It was concluded that when Cu is used as a cathode catalyst, the products of the CO_2 reduction are mainly hydrocarbons (methane, ethene, and ethane) and H_2, while using Ag as the anode resulted mainly in CO and H_2, and much higher CO_2 conversion than for the Cu catalyst. This approach of co-production of value-added chemicals does however hardly fit the requirements of mobility applications like those usually envisaged for direct liquid fuel cells; it is (to the authors' opinion) questionable in principle, because if complex fuels are oxidized, their cost shall counterbalance the interest of the value-added compound generation, the latter reaction usually compromising the overall system performance.

4. Comparison of borohydride, ammonia borane and hydrazine as fuels

In this section borohydride, ammonia borane and hydrazine are compared when investigated as fuels for electrochemical energy production. Their reaction mechanisms on different metals, and the pros and cons for the corresponding direct liquid fuel cells are discussed (Fig. 10). The authors' vision on future developments is also given.

We start by comparing the mechanisms of the BOR, ABOR and HHOR on Pt, Au and Ni, so far being the only metals investigated in sufficient detail. One of the key similarities includes significant dependence of the mechanism of these reactions on the state of the electrode surface (cf. the coverage by O/OH species) since the adsorption of reactive molecules takes place on metal sites. This can be demonstrated in the example of the BOR as depicted in Fig. 10a. On noble metals, complete BH_4^- oxidation usually proceeds only at potentials when the adsorption of OH species is expected (red pathways on Fig. 10a), while at lower potentials the surface is often blocked by $BH_{x,ads}$ species (partially or fully, depending on the potential and number of sites). The behavior of Ni (and likely other non-noble metals) is different in a way that, at

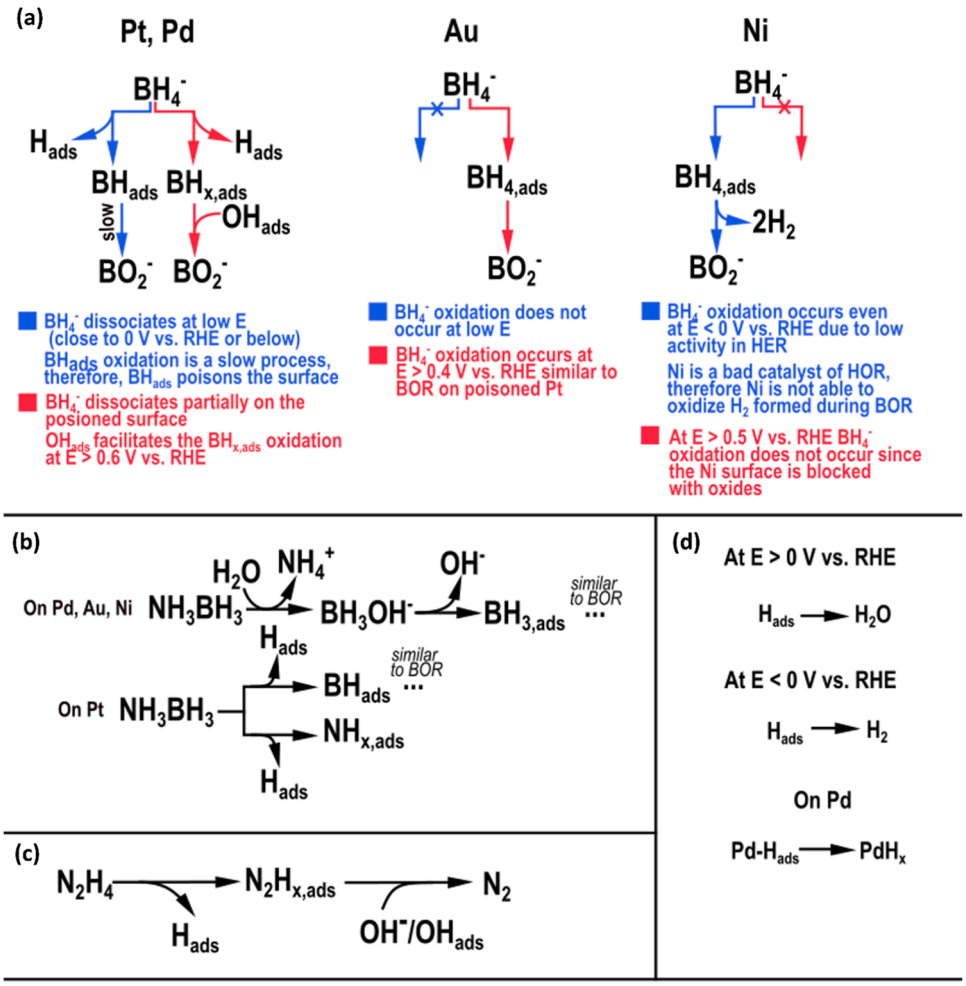

Fig. 10. Schematic representation of the (a) BOR, (b) ABOR, (c) HHOR and (d) H_{ads} valorization on Pt, Pd, Au and Ni in alkaline media. Blue and red colors on panel (a) correspond to the fully metallic surface and the one containing OH_{ads} species, respectively.

practically relevant potentials, the BOR can only proceed on metallic surface, until it is fully blocked with oxides at potentials above ca. 0.5 V vs. RHE. Another important similarity in the mechanism of the BOR, ABOR and HHOR is the formation of the adsorbed hydrogen, which, depending on the strength of M-H bond, can either be oxidized close to 0 (for Pt) or 0.4 V vs. RHE (for Au), absorbed into the bulk of metal (for Pd) or released in a form of H_2 (for metallic Ni). Note that although these steps are mainly observed for the metals mentioned in the parentheses, they can also proceed on the other metals with an impact being dependent on the conditions (cf. OH^- and BH_4^- concentrations, number of sites, potential, pH, T, etc.).

The ABOR mechanism is in general similar to the BOR, except for the first steps as shown in Fig. 10b. On Au, Pd, and Ni the first step must be the B-N bond breaking with the formation of NH_3/NH_4^+ and BH_3OH^-, the latter being oxidized on the surface, likely through the formation of $BH_{x,ads}$. Seemingly, the NH_3-moiety is not valorized during the ABOR in the low potential region, thus leading to a loss of electrons compared to the theoretically expected number. On Pt, the first step of the ABOR might be different, leading to the formation of NH_x species (Fig. 10b), though to the best of the authors' knowledge, there are no studies that clearly demonstrate this. Meanwhile, it must be noted that strong poisoning of Pt surface is expected in the presence of NH_3 based on the literature evidence [216], which however was not observed during the ABOR on Pt.

Although the detailed HHOR mechanism is still not clear, one can conclude that on the discussed metals the reaction proceeds through the formation of $N_2H_{x,ads}$ and H_{ads} following the Eq. (9) and/or (13). The former species can be either oxidized directly by OH^-/OH_{ad} or further dissociate forming H_{ads} (Fig. 10c). The poisoning effect during the HHOR is less pronounced compared to the BOR and ABOR, though to the best of authors' knowledge, there have been no detailed studies devoted to this issue. Meanwhile, since ammonia can be formed following Eqs. (6) and (8), one cannot exclude catalyst poisoning by NH_x species, similar to the case of the ABOR.

Based on the mechanistic discussion presented above, the authors dare to conclude that Au is not a viable perspective for any of the fuels presented in the review, because of the rather high onset potential ($E > 0.4$ V vs. RHE). Pd shows rather good performance but is often struggling from the formation of hydrides, which cannot be oxidized at potentials close to 0 V vs. RHE. This problem cannot be easily solved, which complicates practical implementation of Pd-based catalysts. Both Pt and Ni seem to be a better option for all studied fuels, though some properties still need to be improved. In particular, Pt surface poisoning by BH_{ads} and $NH_{x,ads}$ species at low potentials should be decreased, for example, through alloying it with other metals promoting the formation of OH_{ads} species at low potentials (for example, Ni, Zn, Ce). However, due to the high HER activity of Pt-based catalysts, it is not possible to shift the onset potential of the BOR, ABOR and HHOR significantly below 0 V vs. RHE, leading to non-complete valorization of the fuel energy content. The latter is (more) possible with metallic Ni electrodes, thanks to their very low activity in the HER. However, the (A)BOR mechanism on Ni also involves generation of a significant amount of H_2, thus leading to a loss of electrons. Improving this is important for practical application of Ni catalysts in terms of both power increase and

reduction of the gas production, which can block active sites inside porous electrodes. Besides, since the activity of Ni electrodes is highly sensitive to the presence of NiO_x species on the surface, their concentration should be decreased as much as possible [217]. The latter can be done through alloying of Ni with other metals, like Cu, or introducing metal-support interaction, which opens a very broad area of research.

Regarding the direct liquid fuel cells using the compounds investigated herein, one must confess they all have their pros and cons, making difficult the choice of the "best one". It is true that DBFCs have been under intense focus, even leading to commercial deployment, owing to the high energy and power densities of DBFC systems, including when using non-PGM catalysts; this does not hide the difficulty of recycling the boron oxide products and the complex engineering issues to make BOR sustained in durable anodes, owing to harsh gas formation and precipitation of boron oxides in the anode structure. In addition, one must note that DHHFCs have also been rather well studied and even integrated into vehicles by Daihatsu in the 2000-2010s, the main argument in favor of DHHFCs being the ease of storage/transportation of the hydrazine hydrate and its near-full valorization into gaseous N_2 (a non-toxic and easily eliminated products). This being said, one must state that borane fuel cells have been studied less than DBFCs and DHHFCs. However, the interest of the borane-based fuels is indeed clear, as boranes can be oxidized at lower potential than borohydride on many anode materials, enabling larger cell efficiencies. However, oxidizing the most studied ammonia-borane fuels generates NH_4^+ (hence not fully valorizing the fuel), which is not an easy byproduct to handle, and boron oxides (bringing the same engineering issues than for DBFCs). In the end, for all these systems, developing better anode materials (active, selective and stable), more tolerant cathode materials (to survive in case of fuel crossover, which appears unavoidable), and better separators/membranes is pivotal; having better engineering of the electrodes and of the fuel inlet/outlet loops is also critical. This explains that these devices have only been targeted (except for the Daihatsu study) for niche applications, like aerial/submarine drones or small power electronics. As a matter of fact, there has not been a strong technology driver as was the fuel cell electric vehicles for PEMFCs, and this is possibly the main reason why these direct liquid fuel cells have not been more popular, to date (in addition to the cost of the fuels).

5. Conclusions and outlook

Direct fuel cells fed with carbon-free fuels such as borohydride, ammonia-borane and hydrazine are of interest for portable and mobile applications, where they can be used for safe production of electricity (of particular interest are applications in confined spaces such as submarines). The low thermodynamic potentials and high number of transferred electrons could potentially make them competitive to hydrogen-fed fuel cells. However, currently achieved current and power density is inferior of those reached by state-of-the-art proton exchange membrane fuel cells (PEMFC), which is, to a large extent, due to the anode overpotential resulting from sluggish kinetics of the fuel oxidation reactions. Hence, further efforts are required to develop more efficient anode materials.

This contribution reviewed literature on borohydride, ammonia-borane and hydrazine oxidation with a particular emphasis on recent progress. It shows that the rates of fuel oxidation strongly depend on the composition of the anode, its architecture, pH, and the concentration of the fuel, high concentrations usually resulting in the surface poisoning with strongly adsorbed species. Noble metal-free anode catalysts, notably Ni-based, are very competitive both in half- and full-cell configuration provided that their surface state is thoroughly controlled. Notably, for the BOR, metallic Ni has shown higher (compared to Pt) open circuit voltage due to the fast kinetics of the BOR on its surface, along with an excellent performance in a DBFC. Computational methods (e.g. DFT and microkinetic modeling) have been instrumental in relating the strength of adsorption of the fuel molecule and its fragments and the reaction mechanisms, notably for the BOR.

Bimetallic (e.g. NiM) materials have also been proposed for the oxidation of hydrogen-rich fuels targeting higher activity, selectivity, and tolerance to poisons. However, the role of the second metal (M) remains elusive, and it is often unclear whether it is directly involved in electrocatalysis or rather affects the oxidation state of Ni. Hence, further studies involving *operando* spectroscopies are needed to understand the nature of the active sites to allow the development of advanced catalytic materials.

In what the oxidation products are concerned, borohydride and ammonia-borane oxidation reactions result in borate (BO_2^-) species, whose accumulation in the anode can lead to precipitation in the pores (hence deactivation of the anode) and whose chemical (back) conversion into borohydride is a challenge. In addition, ammonia-borane oxidation leads to ammonia production, since oxidation of the ammonia fragment requires higher overpotential than the borane fragment. In this regard, hydrazine seems to be particularly attractive (despite the fuel toxicity), since its complete oxidation leads to nitrogen and water. It should however be noted that other hydrazine oxidation products (e.g. ammonia) have also been observed. Thus, further studies are required to detect the reaction products (e.g. using DEMS) and unveil how product speciation depends on the type of the catalyst, its surface state, and the reaction conditions in order to propose guidelines for the development of active and selective HHOR catalysts.

Hydrogen escape from these direct fuel cells remains a challenge. It is related to the fuel hydrolysis (notably at high fuel concentrations and the ensuing surface poisoning) and incomplete valorization of hydrogen produced (e.g. during the BOR on Ni due to the mediocre activity of metallic Ni in the hydrogen oxidation reaction).

The authors strongly believe that further progress achieved with the help of *operando* spectroscopic methods (to detect reaction intermediates and determine the nature of the active sites), DEMS (to detect reaction products) and computational methods will allow to develop more potent catalytic materials and further improve the performance of direct fuel cells, making them more competitive and thus attractive for the market.

CRediT authorship contribution statement

Chatenet Marian: Conceptualization, Data curation, Funding acquisition, Investigation, Methodology, Supervision, Validation, Writing – original draft, Writing – review & editing. **Vorms Evgeniia A.:** Investigation, Writing – original draft, Writing – review & editing. **Oshchepkov Alexandr G.:** Conceptualization, Supervision, Writing – original draft, Writing – review & editing. **Bonnefont Antoine:** Conceptualization, Supervision, Validation, Writing – original draft, Writing – review & editing. **Savinova Elena R.:** Conceptualization, Funding acquisition, Supervision, Writing – original draft, Writing – review & editing.

Declaration of Competing Interest

The authors declare that they have no known competing financial interests or personal relationships that could have appeared to influence the work reported in this paper.

Data availability

No data was used for the research described in the article.

Acknowledgements

This work was supported by the Jean-Marie Lehn foundation.

References

[1] J. Łuczak, M. Lieder, Nickel-based catalysts for electrolytic decomposition of ammonia towards hydrogen production, Adv. Colloid Interface Sci. 319 (2023) 102963, https://doi.org/10.1016/j.cis.2023.102963.

[2] Y. Tian, Z. Mao, L. Wang, J. Liang, Green chemistry: advanced electrocatalysts and system design for ammonia oxidation, Small Struct. 4 (2023), https://doi.org/10.1002/sstr.202200266.

[3] P. Zhang, H. Cheng, F. Gu, S. Hong, H. Dong, C. Li, Progress on iron-series metal-organic frameworks materials towards electrocatalytic hydrogen evolution reaction, Surf. Interfaces 42 (2023) 103368, https://doi.org/10.1016/j.surfin.2023.103368.

[4] J.-W. DuanMu, M.-R. Gao, Advances in bio-inspired electrocatalysts for clean energy future, Nano Res. (2023), https://doi.org/10.1007/s12274-023-5977-3.

[5] Y.-H. Wang, F.-Y. Gao, X.-L. Zhang, Y. Yang, J. Liao, Z.-Z. Niu, S. Qin, P.-P. Yang, P.-C. Yu, M. Sun, M.-R. Gao, Efficient NH 3 -tolerant nickel-based hydrogen oxidation catalyst for anion exchange membrane fuel cells, J. Am. Chem. Soc. 145 (2023) 17485–17494, https://doi.org/10.1021/jacs.3c06903.

[6] X.-L. Zhang, P.-C. Yu, X.-Z. Su, S.-J. Hu, L. Shi, Y.-H. Wang, P.-P. Yang, F.-Y. Gao, Z.-Z. Wu, L.-P. Chi, Y.-R. Zheng, M.-R. Gao, Efficient acidic hydrogen evolution in proton exchange membrane electrolyzers over a sulfur-doped marcasite-type electrocatalyst, Sci. Adv. 9 (2023), https://doi.org/10.1126/sciadv.adh2885.

[7] D.R..Lide, CRC Handbook of Chemistry and Physics, 2004.

[8] X.-B. Zhang, S. Han, J.-M. Yan, M. Chandra, H. Shioyama, K. Yasuda, N. Kuriyama, T. Kobayashi, Q. Xu, A new fuel cell using aqueous ammonia-borane as the fuel, J. Power Sour. 168 (2007) 167–171, https://doi.org/10.1016/j.jpowsour.2007.03.009.

[9] S.C. Amendola, P. Onnerud, M.T. Kelly, P.J. Petillo, S.L. Sharp-Goldman, M. Binder, A novel high power density borohydride-air cell, J. Power Sour. 84 (1999) 130–133, https://doi.org/10.1016/S0378-7753(99)00259-1.

[10] E. Gyenge, Electrooxidation of borohydride on platinum and gold electrodes: implications for direct borohydride fuel cells, Electrochim. Acta 49 (2004) 965–978, https://doi.org/10.1016/j.electacta.2003.10.008.

[11] M.H. Atwan, C.L.B. Macdonald, D.O. Northwood, E.L. Gyenge, Colloidal Au and Au-alloy catalysts for direct borohydride fuel cells: Electrocatalysis and fuel cell performance, J. Power Sources 158 (2006) 36–44, https://doi.org/10.1016/j.jpowsour.2005.09.054.

[12] M.H. Atwan, D.O. Northwood, E.L. Gyenge, Evaluation of colloidal Ag and Ag-alloys as anode electrocatalysts for direct borohydride fuel cells, Int. J. Hydrog. Energy 32 (2007) 3116–3125, https://doi.org/10.1016/j.ijhydene.2005.12.022.

[13] M.H. Atwan, E.L. Gyenge, D.O. Northwood, Evaluation of colloidal Pd and Pd-alloys as anode electrocatalysts for direct borohydride fuel cells applications, J. N. Mater. Electrochem. Syst. 13 (2010) 21–27.

[14] M. Atwan, D. Northwood, E.L. Gyenge, Evaluation of colloidal Os and Os-Alloys (Os–Sn, Os–Mo and Os–V) for electrocatalysis of methanol and borohydride oxidation, Int. J. Hydrog. Energy 30 (2005) 1323–1331, https://doi.org/10.1016/j.ijhydene.2005.04.010.

[15] E. Gyenge, M. Atwan, D. Northwood, Electrocatalysis of borohydride oxidation on colloidal Pt and Pt-Alloys (Pt-Ir, Pt-Ni, and Pt-Au) and application for direct borohydride fuel cell anodes, J. Electrochem. Soc. 153 (2006) A150, https://doi.org/10.1149/1.2131831.

[16] M. Chatenet, F. Micoud, I. Roche, E. Chainet, Kinetics of sodium borohydride direct oxidation and oxygen reduction in sodium hydroxide electrolyte, Electrochim. Acta 51 (2006) 5459–5467, https://doi.org/10.1016/j.electacta.2006.02.015.

[17] M. Simões, S. Baranton, C. Coutanceau, Electrooxidation of sodium borohydride at Pd, Au, and Pd x Au 1− x carbon-supported nanocatalysts, J. Phys. Chem. C. 113 (2009) 13369–13376, https://doi.org/10.1021/jp902741z.

[18] M. Simões, S. Baranton, C. Coutanceau, Influence of bismuth on the structure and activity of Pt and Pd nanocatalysts for the direct electrooxidation of NaBH4, Electrochim. Acta 56 (2010) 580–591, https://doi.org/10.1016/j.electacta.2010.09.006.

[19] C. Grimmer, R. Zacharias, M. Grandi, B. Cermenek, A. Schenk, S. Weinberger, F.-A. Mautner, B. Bitschnau, V. Hacker, Carbon supported ruthenium as anode catalyst for alkaline direct borohydride fuel cells, J. Phys. Chem. C. 119 (2015) 23839–23844, https://doi.org/10.1021/acs.jpcc.5b06862.

[20] C. Grimmer, M. Grandi, R. Zacharias, B. Cermenek, H. Weber, C. Morais, T. W. Napporn, S. Weinberger, A. Schenk, V. Hacker, The electrooxidation of borohydride: a mechanistic study on palladium (Pd/C) applying RRDE, ^{11}B NMR and FTIR, Appl. Catal. B Environ. 180 (2016) 614–621, https://doi.org/10.1016/j.apcatb.2015.07.028.

[21] G. Backović, J. Milikić, S. De Negri, A. Saccone, B. Šljukić, D.M.F. Santos, Enhanced borohydride oxidation kinetics at gold-rare earth alloys, J. Alloy. Compd. 857 (2021) 158273, https://doi.org/10.1016/j.jallcom.2020.158273.

[22] B. Šljukić, J. Milikić, D.M.F. Santos, C.A.C. Sequeira, D. Macciò, A. Saccone, Electrocatalytic performance of Pt–Dy alloys for direct borohydride fuel cells, J. Power Sour. 272 (2014) 335–343, https://doi.org/10.1016/j.jpowsour.2014.08.080.

[23] M. Martins, B. Šljukić, Ö. Metin, M. Sevim, C.A.C. Sequeira, T. Şener, D.M. F. Santos, Bimetallic PdM (M = Fe, Ag, Au) alloy nanoparticles assembled on reduced graphene oxide as catalysts for direct borohydride fuel cells, J. Alloy. Compd. 718 (2017) 204–214, https://doi.org/10.1016/j.jallcom.2017.05.058.

[24] R.L. Arevalo, M.C.S. Escaño, H. Kasai, Computational mechanistic study of borohydride electrochemical oxidation on Au 3 Ni(111), J. Phys. Chem. C. 117 (2013) 3818–3825, https://doi.org/10.1021/jp311904k.

[25] M.C.S. Escaño, E. Gyenge, R.L. Arevalo, H. Kasai, Reactivity descriptors for borohydride interaction with metal surfaces, J. Phys. Chem. C. 115 (2011) 19883–19889, https://doi.org/10.1021/jp207768e.

[26] G. Rostamikia, M.J. Janik, First principles mechanistic study of borohydride oxidation over the Pt(111) surface, Electrochim. Acta 55 (2010) 1175–1183, https://doi.org/10.1016/j.electacta.2009.10.002.

[27] G. Rostamikia, M.J. Janik, Borohydride oxidation over Au(111): a first-principles mechanistic study relevant to direct borohydride fuel cells, J. Electrochem. Soc. 156 (2009) B86, https://doi.org/10.1149/1.3010382.

[28] M.C.S. Escaño, R.L. Arevalo, E. Gyenge, H. Kasai, Electrocatalysis of borohydride oxidation: a review of density functional theory approach combined with experimental validation, J. Phys. Condens. Matter 26 (2014) 353001, https://doi.org/10.1088/0953-8984/26/35/353001.

[29] D.A. Finkelstein, C.D. Letcher, D.J. Jones, L.M. Sandberg, D.J. Watts, H. D. Abruña, Self-poisoning during BH 4 – oxidation at Pt and Au, and in situ poison removal procedures for BH 4 – Fuel Cells, J. Phys. Chem. C. 117 (2013) 1571–1581, https://doi.org/10.1021/jp308677f.

[30] M.C.S. Escaño, Borohydride electro-oxidation on metal electrodes: structure, composition and solvent effects from DFT, SPR Electrochem 14 (2017) 1–22, https://doi.org/10.1039/9781782622727-00001.

[31] A.G. Oshchepkov, G. Braesch, S. Ould-Amara, G. Rostamikia, G. Maranzana, A. Bonnefont, V. Papaefthimiou, M.J. Janik, M. Chatenet, E.R. Savinova, Nickel metal nanoparticles as anode electrocatalysts for highly efficient direct borohydride fuel cells, ACS Catal. 9 (2019) 8520–8528, https://doi.org/10.1021/acscatal.9b01616.

[32] P. Ferrin, S. Kandoi, A.U. Nilekar, M. Mavrikakis, Hydrogen adsorption, absorption and diffusion on and in transition metal surfaces: a DFT study, Surf. Sci. 606 (2012) 679–689, https://doi.org/10.1016/j.susc.2011.12.017.

[33] S.-C. Huang, C.-H. Lin, J.-H. Wang, Trends of water gas shift reaction on close-packed transition metal surfaces, J. Phys. Chem. C. 114 (2010) 9826–9834, https://doi.org/10.1021/jp1005814.

[34] V. Briega-Martos, E. Herrero, J.M. Feliu, Borohydride electro-oxidation on Pt single crystal electrodes, Electrochem. Commun. 51 (2015) 144–147, https://doi.org/10.1016/j.elecom.2014.12.024.

[35] H. Qin, K. Chen, C. Zhu, J. Liu, J. Wang, Y. He, H. Chi, H. Ni, Z. Ji, High electrocatalytic activity for borohydride oxidation on palladium nanocubes enclosed by {200} facets, J. Power Sources 299 (2015) 241–245, https://doi.org/10.1016/j.jpowsour.2015.09.007.

[36] P.-Y. Olu, B. Gilles, N. Job, M. Chatenet, Influence of the surface morphology of smooth platinum electrodes for the sodium borohydride oxidation reaction, Electrochem. Commun. 43 (2014) 47–50, https://doi.org/10.1016/j.elecom.2014.02.018.

[37] P.-Y. Olu, C.R. Barros, N. Job, M. Chatenet, Electrooxidation of NaBH4 in alkaline medium on well-defined Pt nanoparticles deposited onto flat glassy carbon substrate: evaluation of the effects of Pt nanoparticle size, inter-particle distance, and loading, Electrocatalysis 5 (2014) 288–300, https://doi.org/10.1007/s12678-014-0195-0.

[38] V.L. Oliveira, E. Sibert, Y. Soldo-Olivier, E.A. Ticianelli, M. Chatenet, Investigation of the electrochemical oxidation reaction of the borohydride anion in palladium layers on Pt(111), Electrochim. Acta 209 (2016) 360–368, https://doi.org/10.1016/j.electacta.2016.05.093.

[39] Z. Jusys, R.J. Behm, Borohydride electrooxidation over Pt/C, AuPt/C and Au/C catalysts: partial reaction pathways and mixed potential formation, Electrochem. Commun. 60 (2015) 9–12, https://doi.org/10.1016/j.elecom.2015.07.021.

[40] M. Chatenet, M.B. Molina-Concha, J.-P. Diard, First insights into the borohydride oxidation reaction mechanism on gold by electrochemical impedance spectroscopy, Electrochim. Acta 54 (2009) 1687–1693, https://doi.org/10.1016/j.electacta.2008.09.060.

[41] G. Parrour, M. Chatenet, J.-P. Diard, Electrochemical impedance spectroscopy study of borohydride oxidation reaction on gold—towards a mechanism with two electrochemical steps, Electrochim. Acta 55 (2010) 9113–9124, https://doi.org/10.1016/j.electacta.2010.07.086.

[42] P. Krishnan, T.-H. Yang, S.G. Advani, A.K. Prasad, Rotating ring-disc electrode (RRDE) investigation of borohydride electro-oxidation, J. Power Sources 182 (2008) 106–111, https://doi.org/10.1016/j.jpowsour.2008.03.064.

[43] D.A. Finkelstein, N.Da Mota, J.L. Cohen, H.D. Abruña, Rotating disk electrode (RDE) investigation of BH 4 − and BH 3 OH − electro-oxidation at Pt and Au: implications for BH 4 − fuel cells, J. Phys. Chem. C. 113 (2009) 19700–19712, https://doi.org/10.1021/jp900933c.

[44] M. Chatenet, F.H.B. Lima, E.A. Ticianelli, Gold is not a faradaic-efficient borohydride oxidation electrocatalyst: an online electrochemical mass spectrometry study, J. Electrochem. Soc. 157 (2010) B697, https://doi.org/10.1149/1.3328179.

[45] F.H.B. Lima, A.M. Pasqualeti, M.B. Molina Concha, M. Chatenet, E.A. Ticianelli, Borohydride electrooxidation on Au and Pt electrodes, Electrochim. Acta 84 (2012) 202–212, https://doi.org/10.1016/j.electacta.2012.05.030.

[46] A.M. Pasqualeti, P.-Y. Olu, M. Chatenet, F.H.B. Lima, Borohydride electrooxidation on carbon-supported noble metal nanoparticles: insights into hydrogen and hydroxyborane formation, ACS Catal. 5 (2015) 2778–2787, https://doi.org/10.1021/acscatal.5b00107.

[47] B.M. Concha, M. Chatenet, F. Maillard, E.A. Ticianelli, F.H.B. Lima, R.B. de Lima, In situ infrared (FTIR) study of the mechanism of the borohydride oxidation reaction, Phys. Chem. Chem. Phys. 12 (2010) 11507, https://doi.org/10.1039/c003652h.

[48] B. Molina Concha, M. Chatenet, E.A. Ticianelli, F.H.B. Lima, In situ infrared (FTIR) study of the mechanism of the borohydride oxidation reaction on smooth

Pt electrode, J. Phys. Chem. C. 115 (2011) 12439–12447, https://doi.org/10.1021/jp2002589.
[49] G. Braesch, A. Bonnefont, V. Martin, E.R. Savinova, M. Chatenet, Borohydride oxidation reaction mechanisms and poisoning effects on Au, Pt and Pd bulk electrodes: From model (low) to direct borohydride fuel cell operating (high) concentrations, Electrochim. Acta 273 (2018) 483–494, https://doi.org/10.1016/j.electacta.2018.04.068.
[50] P.-Y. Olu, A. Bonnefont, G. Braesch, V. Martin, E.R. Savinova, M. Chatenet, Influence of the concentration of borohydride towards hydrogen production and escape for borohydride oxidation reaction on Pt and Au electrodes – experimental and modelling insights, J. Power Sources 375 (2018) 300–309, https://doi.org/10.1016/j.jpowsour.2017.07.061.
[51] C. Lafforgue, R.W. Atkinson, K. Swider-Lyons, M. Chatenet, Evaluation of carbon-supported palladium electrocatalysts for the borohydride oxidation reaction in conditions relevant to fuel cell operation, Electrochim. Acta 341 (2020) 135971, https://doi.org/10.1016/j.electacta.2020.135971.
[52] Ş. Karabiberoğlu, Z. Dursun, Au-Pt bimetallic nanoparticles anchored on conducting polymer: an effective electrocatalyst for direct electrooxidation of sodium borohydride in alkaline solution, Mater. Sci. Eng. B. 288 (2023) 116158, https://doi.org/10.1016/j.mseb.2022.116158.
[53] C.K. Raul, S. Dey, M. Halder, R. Karmakar, S. Basu, A.K. Meikap, Synthesis of AuxCo100 − x/MWCNT nanoparticles as an efficient anode electrocatalyst for borohydride oxidation in alkaline medium, J. Appl. Electrochem. 53 (2023) 977–990, https://doi.org/10.1007/s10800-022-01824-5.
[54] K.S. Freitas, B.M. Concha, E.A. Ticianelli, M. Chatenet, Mass transport effects in the borohydride oxidation reaction—Influence of the residence time on the reaction onset and faradaic efficiency, Catal. Today 170 (2011) 110–119, https://doi.org/10.1016/j.cattod.2011.01.051.
[55] N. Saxena, N.V.S. Praneeth, K.J. Rao, S. Paria, Organization of palladium nanoparticles into fractal patterns for highly enhanced catalytic activity and anode material for direct borohydride fuel cells applications, ACS Appl. Energy Mater. 1 (2018) 2164–2175, https://doi.org/10.1021/acsaem.8b00211.
[56] H. Zhang, S. Liu, Z. Wang, X. Li, K. Deng, H. Yu, X. Wang, Y. Xu, H. Wang, L. Wang, Ni-doped hyperbranched PdCu nanocrystals for efficient electrocatalytic borohydride oxidation, J. Mater. Chem. A. 10 (2022) 24694–24700, https://doi.org/10.1039/D2TA07066A.
[57] L.C. Nagle, J.F. Rohan, Nanoporous gold anode catalyst for direct borohydride fuel cell, Int. J. Hydrog. Energy 36 (2011) 10319–10326, https://doi.org/10.1016/j.ijhydene.2010.09.077.
[58] J.P. Elder, A. Hickling, Anodic behaviour of the borohydride ion, Trans. Faraday Soc. 58 (1962) 1852–1864.
[59] B.H. Liu, Z.P. Li, S. Suda, Anodic oxidation of alkali borohydrides catalyzed by nickel, J. Electrochem. Soc. 150 (2003) A398, https://doi.org/10.1149/1.1553785.
[60] B.H. Liu, Z.P. Li, S. Suda, Electrocatalysts for the anodic oxidation of borohydrides, Electrochim. Acta 49 (2004) 3097–3105, https://doi.org/10.1016/j.electacta.2004.02.023.
[61] K. Wang, J. Lu, L. Zhuang, A current−decomposition study of the borohydride oxidation reaction at Ni electrodes, J. Phys. Chem. C. 111 (2007) 7456–7462, https://doi.org/10.1021/jp0710483.
[62] B.H. Liu, Z.P. Li, S. Suda, Development of high-performance planar borohydride fuel cell modules for portable applications, J. Power Sources 175 (2008) 226–231, https://doi.org/10.1016/j.jpowsour.2007.09.047.
[63] J. Ma, Y. Sahai, R.G. Buchheit, Direct borohydride fuel cell using Ni-based composite anodes, J. Power Sources 195 (2010) 4709–4713, https://doi.org/10.1016/j.jpowsour.2010.02.034.
[64] R. Mahmoodi, M.G. Hosseini, H. Rasouli, Enhancement of output power density and performance of direct borohydride-hydrogen peroxide fuel cell using Ni-Pd core-shell nanoparticles on polymeric composite supports (rGO-PANI) as novel electrocatalysts, Appl. Catal. B Environ. 251 (2019) 37–48, https://doi.org/10.1016/j.apcatb.2019.03.064.
[65] B. Šljukić, M. Martins, E. Kayhan, A. Balčiūnaitė, T. Şener, C.A.C. Sequeira, D.M. F. Santos, SnO2-C supported PdNi nanoparticles for oxygen reduction and borohydride oxidation, J. Electroanal. Chem. 797 (2017) 23–30, https://doi.org/10.1016/j.jelechem.2017.05.013.
[66] D. Cao, Y. Gao, G. Wang, R. Miao, Y. Liu, A direct $NaBH_4$–H_2O_2 fuel cell using Ni foam supported Au nanoparticles as electrodes, Int. J. Hydrog. Energy 35 (2010) 807–813, https://doi.org/10.1016/j.ijhydene.2009.11.026.
[67] X. Ma, K. Ye, G. Wang, M. Duan, K. Cheng, G. Wang, D. Cao, Facile fabrication of gold coated nickel nanoarrays and its excellent catalytic performance towards sodium borohydride electro-oxidation, Appl. Surf. Sci. 414 (2017) 353–360, https://doi.org/10.1016/j.apsusc.2017.04.104.
[68] L. Tamašauskaitė-Tamašiūnaitė, A. Balčiūnaitė, D. Šimkūnaitė, A. Selskis, Self-ordered titania nanotubes and flat surfaces as a support for the deposition of nanostructured Au–Ni catalyst: enhanced electrocatalytic oxidation of borohydride, J. Power Sources 202 (2012) 85–91, https://doi.org/10.1016/j.jpowsour.2011.11.030.
[69] D. Duan, J. Liang, H. Liu, X. You, H. Wei, G. Wei, S. Liu, The effective carbon supported core-shell structure of Ni@Au catalysts for electro-oxidation of borohydride, Int. J. Hydrog. Energy 40 (2015) 488–500, https://doi.org/10.1016/j.ijhydene.2014.10.101.
[70] M. Martins, B. Šljukić, C.A.C. Sequeira, G.S.P. Soylu, A.B. Yurtcan, G. Bozkurt, T. Sener, D.M.F. Santos, PtNi supported on binary metal oxides: Potential bifunctional electrocatalysts for low-temperature fuel cells, Appl. Surf. Sci. 428 (2018) 31–40, https://doi.org/10.1016/j.apsusc.2017.09.132.
[71] B. Šljukić, J. Milikić, D.M.F. Santos, C.A.C. Sequeira, Carbon-supported Pt0.75M0.25 (M = Ni or Co) electrocatalysts for borohydride oxidation, Electrochim. Acta 107 (2013) 577–583, https://doi.org/10.1016/j.electacta.2013.06.040.
[72] L. Tamasauskaite-Tamasiunaite, A. Balčiunaite, A. Zabielaite, J. Vaičiuniene, A. Selskis, V. Pakštas, E. Norkus, Electrocatalytic activity of nanostructured Pt-Ni catalysts deposited on the titania nanotube arrays towards borohydride oxidation, J. Electroanal. Chem. 707 (2013) 31–37, https://doi.org/10.1016/j.jelechem.2013.08.025.
[73] M. Martins, J. Milikić, B. Šljukić, G.S.P. Soylu, A.B. Yurtcan, G. Bozkurt, D.M. F. Santos, Mn2O3-MO (MO = ZrO2, V2O5, WO3) supported PtNi nanoparticles: designing stable and efficient electrocatalysts for oxygen reduction and borohydride oxidation, Microporous Mesoporous Mater. 273 (2019) 286–293, https://doi.org/10.1016/j.micromeso.2018.07.022.
[74] M. Hasan, S.B. Newcomb, K.M. Razeeb, Novel core/shell Ni@NiO/Pt as high efficient electrocatalyst for alkaline direct ethanol fuel cells, ECS Trans. 45 (2013) 111–126, https://doi.org/10.1149/04520.0111ecst.
[75] V.A. Grinberg, N.A. Mayorova, A.A. Korlyukov, A.A. Pasynskii, Direct borohydride oxidation electrocatalysts based on Ni-Ru/C and Ni-Ru-F/C alloys, Russ. J. Electrochem. 46 (2010) 1289–1296, https://doi.org/10.1134/S1023193510110091.
[76] B. Li, Q. Yan, C. Song, P. Yan, K. Ye, K. Cheng, K. Zhu, J. Yan, D. Cao, G. Wang, Reduced graphene oxide foam supported CoNi nanosheets as an efficient anode catalyst for direct borohydride hydrogen peroxide fuel cell, Appl. Surf. Sci. 491 (2019) 659–669, https://doi.org/10.1016/j.apsusc.2019.06.110.
[77] S. Saha, S. Ganguly, D. Banerjee, K. Kargupta, Novel bimetallic graphene-cobalt-nickel (G-Co-Ni) nano-ensemble electrocatalyst for enhanced borohydride oxidation, Int. J. Hydrog. Energy 40 (2015) 1760–1773, https://doi.org/10.1016/j.ijhydene.2014.11.143.
[78] M. Guo, Y. Cheng, Y. Yu, J. Hu, Ni-Co nanoparticles immobilized on a 3D Ni foam template as a highly efficient catalyst for borohydride electrooxidation in alkaline medium, Appl. Surf. Sci. 416 (2017) 439–445, https://doi.org/10.1016/j.apsusc.2017.04.193.
[79] D.M.F. Santos, S. Eugénio, D.S.P. Cardoso, B. Šljukić, M.F. Montemor, Three-dimensional nanostructured Ni-Cu foams for borohydride oxidation, Russ. J. Phys. Chem. A. 89 (2015) 2449–2454, https://doi.org/10.1134/S0036024415130336.
[80] C. Song, G. Wang, B. Li, C. Miao, K. Ma, K. Zhu, K. Cheng, K. Ye, J. Yan, D. Cao, J. Yin, A novel electrode of ternary CuNiPd nanoneedles decorated Ni foam and its catalytic activity toward NaBH 4 electrooxidation, Electrochim. Acta 299 (2019) 395–404, https://doi.org/10.1016/j.electacta.2018.12.185.
[81] C. Wu, J. Zhu, H. Wang, G. Wang, T. Chen, Y. Tan, Porous Ni 1– x Cu x O nanowire arrays as noble-metal-free high-performance catalysts for ammonia-borane electrooxidation, ACS Catal. 10 (2020) 721–735, https://doi.org/10.1021/acscatal.9b03809.
[82] E.A. Vorms, E.A. Suprun, A.V. Nartova, R.I. Kvon, A.G. Oshchepkov, Electrodeposited NiCu nanoparticles for the borohydride oxidation reaction: effect of Cu on the activity and stability of Ni upon surface oxidation, Electrochim. Acta 433 (2022) 141196, https://doi.org/10.1016/j.electacta.2022.141196.
[83] B. Hu, J. Yu, J. Meng, C. Xu, J. Cai, B. Zhang, Y. Liu, D. Yu, X. Zhou, C. Chen, Porous Ni–Cu alloy dendrite anode catalysts with high activity and selectivity for direct borohydride fuel cells, ACS Appl. Mater. Interfaces 14 (2022) 3910–3918, https://doi.org/10.1021/acsami.1c15671.
[84] B.H. Liu, S. Suda, Hydrogen storage alloys as the anode materials of the direct borohydride fuel cell, J. Alloy. Compd. 454 (2008) 280–285, https://doi.org/10.1016/j.jallcom.2006.12.034.
[85] W.J. Paschoalino, E.A. Ticianelli, An investigation of the borohydride oxidation reaction on La-Ni-based hydrogen storage alloys, Int. J. Hydrog. Energy 38 (2013) 7344–7352, https://doi.org/10.1016/j.ijhydene.2013.04.036.
[86] D.M.F. Santos, B. Šljukić, L. Amaral, D. Macciò, A. Saccone, C.A.C. Sequeira, Nickel and nickel-cerium alloy anodes for direct borohydride fuel cells, J. Electrochem. Soc. 161 (2014) F594–F599, https://doi.org/10.1149/2.023405jes.
[87] D.M.F. Santos, B. Šljukić, L. Amaral, J. Milikić, C.A.C. Sequeira, D. Macciò, A. Saccone, Nickel-rare earth electrodes for sodium borohydride electrooxidation, Electrochim. Acta 190 (2016) 1050–1056, https://doi.org/10.1016/j.electacta.2015.12.218.
[88] R.P. Šimpraga, Reversibility and irreversibility in the formation and reduction of oxide film states on Co at ambient and low temperatures, J. Electroanal. Chem. 355 (1993) 79–96, https://doi.org/10.1016/0022-0728(93)80355-L.
[89] F. Reikowski, F. Maroun, N. Di, P. Allongue, M. Ruge, J. Stettner, O. M. Magnussen, In situ surface X-ray diffraction study of ultrathin epitaxial Co films on Au(111) in alkaline solution, Electrochim. Acta 197 (2016) 273–281, https://doi.org/10.1016/j.electacta.2016.01.052.
[90] G. Rostamikia, R.J. Patel, I. Merino-Jimenez, M. Hickner, M.J. Janik, Electrocatalyst design for direct borohydride oxidation guided by first principles, J. Phys. Chem. C. 121 (2017) 2872–2881, https://doi.org/10.1021/acs.jpcc.6b12159.
[91] D. Duan, H. Liu, X. You, H. Wei, S. Liu, Anodic behavior of carbon supported Cu@Ag core-shell nanocatalysts in direct borohydride fuel cells, J. Power Sources 293 (2015) 292–300, https://doi.org/10.1016/j.jpowsour.2015.05.086.
[92] M.R.G. De Chialvo, S.L. Marchiano, A.J. Arvía, The mechanism of oxidation of copper in alkaline solutions, J. Appl. Electrochem. 14 (1984) 165–175, https://doi.org/10.1007/BF00618735.

[93] J. Cai, P. Chen, B. Hu, C. Xu, Y. Yang, J. Meng, B. Zhang, C. Chen, D. Yu, X. Zhou, Succulent-plant-like Ni–Co alloy efficient catalysts for direct borohydride fuel cells, Dalt. Trans. 52 (2023) 1378–1387, https://doi.org/10.1039/D2DT03656H.
[94] S. Guo, J. Sun, Z. Zhang, A. Sheng, M. Gao, Z. Wang, B. Zhao, W. Ding, Study of the electrooxidation of borohydride on a directly formed CoB / Ni-foam electrode and its application in membraneless direct borohydride, (2017) 15879–15890. https://doi.org/10.1039/c7ta03464d.
[95] Z. Wu, X. Mao, Q. Zi, R. Zhang, T. Dou, A.C.K. Yip, Mechanism and kinetics of sodium borohydride hydrolysis over crystalline nickel and nickel boride and amorphous nickel–boron nanoparticles, J. Power Sources 268 (2014) 596–603, https://doi.org/10.1016/j.jpowsour.2014.06.067.
[96] A. Oshchepkov, A. Bonnefont, G. Maranzana, E.R. Savinova, M. Chatenet, Direct borohydride fuel cells: a selected review of their reaction mechanisms, electrocatalysts, and influence of operating parameters on their performance, Curr. Opin. Electrochem. 32 (2022) 100883, https://doi.org/10.1016/j.coelec.2021.100883.
[97] M.G. Hosseini, M. Abdolmaleki, F. Nasirpouri, Investigation of the porous nanostructured Cu/Ni/AuNi electrode for sodium borohydride electrooxidation, Electrochim. Acta 114 (2013) 215–222, https://doi.org/10.1016/j.electacta.2013.10.012.
[98] A.G. Oshchepkov, G. Braesch, G. Rostamikia, A. Bonnefont, M.J. Janik, M. Chatenet, E.R. Savinova, Insights into the borohydride electrooxidation reaction on metallic nickel from operando FTIRS, on-line DEMS and DFT, Electrochim. Acta 389 (2021) 138721, https://doi.org/10.1016/j.electacta.2021.138721.
[99] D. Zhang, K. Cheng, N. Shi, F. Guo, G. Wang, D. Cao, Nickel particles supported on multi-walled carbon nanotubes modified sponge for sodium borohydride electrooxidation, Electrochem. Commun. 35 (2013) 128–130, https://doi.org/10.1016/j.elecom.2013.08.015.
[100] V.O. Romanova, A.V. Romanov, A.V. Churikov, I.M. Gamayunova, M. A. Churikov, Electrochemical oxidation of borohydride-ion on nickel electrode: a study by the method of IR-spectroscopy, Electrochem. Energ 14 (2014) 57–67.
[101] O.A. Sadik, H. Xu, A. Sargent, Multi-electron transfer mechanism of dimethylamine borane in electroless gold deposition, J. Electroanal. Chem. 583 (2005) 167–175, https://doi.org/10.1016/j.jelechem.2005.05.013.
[102] A.G. Oshchepkov, P.A. Simonov, O.V. Cherstiouk, R.R. Nazmutdinov, D. V. Glukhov, V.I. Zaikovskii, T.Y. Kardash, R.I. Kvon, A. Bonnefont, A.N. Simonov, V.N. Parmon, E.R. Savinova, On the effect of Cu on the activity of carbon supported Ni nanoparticles for hydrogen electrode reactions in alkaline medium, Top. Catal. 58 (2015) 1181–1192, https://doi.org/10.1007/s11244-015-0487-5.
[103] B. Hu, Y. Xie, Y. Yang, J. Meng, J. Cai, C. Chen, D. Yu, X. Zhou, Boosting borohydride oxidation by control lattice-strain of Ni@NiP electrocatalyst with core-shell structure, Appl. Catal. B Environ. 324 (2023) 122257, https://doi.org/10.1016/j.apcatb.2022.122257.
[104] L.C. Nagle, J.F. Rohan, Ammonia borane oxidation at gold microelectrodes in alkaline solutions, J. Electrochem. Soc. 153 (2006) C773, https://doi.org/10.1149/1.2344842.
[105] S. Pylypko, A. Zadick, M. Chatenet, P. Miele, M. Cretin, U.B. Demirci, A preliminary study of sodium octahydrotriborate NaB3H8 as potential anodic fuel of direct liquid fuel cell, J. Power Sources 286 (2015) 10–17, https://doi.org/10.1016/j.jpowsour.2015.03.143.
[106] S. Pylypko, S. Ould-Amara, A. Zadick, E. Petit, M. Chatenet, M. Cretin, U. B. Demirci, The highly stable aqueous solution of sodium dodecahydro- closo -dodecaborate Na 2 B 12H 12 as a potential liquid anodic fuel, Appl. Catal. B Environ. 222 (2018) 1–8, https://doi.org/10.1016/j.apcatb.2017.09.068.
[107] A. Sargent, O.A. Sadik, L.J. Matienzo, Probing the mechanism of electroless gold plating using an electrochemical quartz crystal microbalance I. Elucidating the nature of reactive intermediates in dimethylamine borane, J. Electrochem. Soc. 148 (2001) C257, https://doi.org/10.1149/1.1353572.
[108] T. Homma, A. Tamaki, H. Nakai, T. Osaka, Molecular orbital study on the reaction process of dimethylamine borane as a reductant for electroless deposition, J. Electroanal. Chem. 559 (2003) 131–136, https://doi.org/10.1016/S0022-0728(03)00042-1.
[109] D. Plana, R.A.W. Dryfe, The electro-oxidation of dimethylamine borane: part 1, polycrystalline substrates, Electrochim. Acta 56 (2011) 3835–3844, https://doi.org/10.1016/j.electacta.2011.02.041.
[110] D. Plana, P. Rodriguez, M.T.M. Koper, R.A.W. Dryfe, The electro-oxidation of dimethylamine borane: part 2, in situ FTIR on single-crystal gold electrodes, Electrochim. Acta 56 (2011) 7637–7643, https://doi.org/10.1016/j.electacta.2011.06.072.
[111] M. Belén Molina Concha, M. Chatenet, F.H.B. Lima, E.A. Ticianelli, In situ Fourier transform infrared spectroscopy and on-line differential electrochemical mass spectrometry study of the NH3BH3 oxidation reaction on gold electrodes, Electrochim. Acta 89 (2013) 607–615, https://doi.org/10.1016/j.electacta.2012.11.027.
[112] D. Barsuk, A. Zadick, M. Chatenet, K. Georgarakis, N.T. Panagiotopoulos, Y. Champion, A. Moreira Jorge, Nanoporous silver for electrocatalysis application in alkaline fuel cells, Mater. Des. 111 (2016) 528–536, https://doi.org/10.1016/j.matdes.2016.09.037.
[113] J. Luo, P. Han, Z. Dan, F. Qin, T. Tang, Y. Dong, Bimodal nanoporous silver fabricated from dual-phase Ag10Zn90 precursor via electrochemical dealloying for direct ammonia-borane electrooxidation, Microporous Mesoporous Mater. 308 (2020) 110532, https://doi.org/10.1016/j.micromeso.2020.110532.
[114] L.C. Nagle, J.F. Rohan, Nanoporous gold catalyst for direct ammonia borane fuel cells, J. Electrochem. Soc. 158 (2011) B772–B778, https://doi.org/10.1149/1.3583637.
[115] A. Zadick, J.-F. Petit, V. Martin, L. Dubau, U.B. Demirci, C. Geantet, M. Chatenet, Ubiquitous borane fuel electrooxidation on Pd/C and Pt/C electrocatalysts: toward promising direct hydrazine–borane fuel cells, ACS Catal. 8 (2018) 3150–3163, https://doi.org/10.1021/acscatal.7b04321.
[116] B. Filanovsky, E. Granot, R. Dirawi, I. Presman, I. Kuras, F. Patolsky, Nanotextured metal copper substrates as powerful and long-lasting fuel cell anodes, Nano Lett. 11 (2011) 1727–1732, https://doi.org/10.1021/nl200282z.
[117] A. Zadick, L. Dubau, K. Artyushkova, A. Serov, P. Atanassov, M. Chatenet, Nickel-based electrocatalysts for ammonia borane oxidation: enabling materials for carbon-free-fuel direct liquid alkaline fuel cell technology, Nano Energy 37 (2017) 248–259, https://doi.org/10.1016/j.nanoen.2017.05.035.
[118] J. Yu, H. Jing, P. Zhao, K. Lu, J. Song, Z. Wu, H. Wu, B. Liu, W. Lei, Q. Hao, Defect-rich walnut-like copper-doped Ni(PO3)2 catalyst towards ammonia borane electrooxidation reaction with high performance, J. Mater. Chem. A. 10 (2022) 2035–2044, https://doi.org/10.1039/D1TA09483A.
[119] G. Wang, H. Wang, T. Chen, Y. Tan, Ni1−xMxSe2 (M = Fe, Co, Cu) nanowires as anodes for ammonia-borane electrooxidation and the derived Ni1−xMxSe2−y –OOH ultrathin nanosheets as efficient electrocatalysts for oxygen evolution, J. Mater. Chem. A. 7 (2019) 16372–16386, https://doi.org/10.1039/C9TA04681J.
[120] R. Miao, R.G. Compton, The electro-oxidation of hydrazine: a self-inhibiting reaction, J. Phys. Chem. Lett. 12 (2021) 1601–1605, https://doi.org/10.1021/acs.jpclett.1c00070.
[121] J. Heitbaum, W. Vielstich, Untersuchungen zur anodischen oxidation des hydrazins im alkalischen elektrolyten—I. Der reaktionsmechanismus an platinelektroden, Electrochim. Acta 18 (1973) 501–507, https://doi.org/10.1016/0013-4686(73)80055-6.
[122] N.V. Korovin, Hydrazine, Chimiya, Moscow, 1980.
[123] T.O. Pavela, No Title, Suom. Kemistil. 30B (1957) 240.
[124] D.A. Finkelstein, R. Imbeault, S. Garbarino, L. Roué, D. Guay, Trends in catalysis and catalyst cost effectiveness for N 2H 4 fuel cells and sensors: a rotating disk electrode (RDE) study, J. Phys. Chem. C. 120 (2016) 4717–4738, https://doi.org/10.1021/acs.jpcc.5b10156.
[125] M. Gutjahr, W. Vielstich, Zur anodischen Oxidation von Hydrazin in alkalischem Elektrolyten, Chem. Ing. Tech. - CIT 40 (1968) 180–185, https://doi.org/10.1002/cite.330400408.
[126] N.V. Korovin, B.N. Yanchuk, Hydrogen sorption by palladium in hydrazine electro-oxidation, Electrochim. Acta 15 (1970) 569–580, https://doi.org/10.1016/0013-4686(70)80008-1.
[127] Y. Fukumoto, T. Matsunaga, T. Hayashi, Electrocatalytic activities of metal electrodes in anodic oxidation of hydrazine in alkaline solution, Electrochim. Acta 26 (1981) 631–636, https://doi.org/10.1016/0013-4686(81)80031-X.
[128] J.A. Harrison, Z.A. Khan, The oxidation of hydrazine in alkaline solution at platinum and mercury, J. Electroanal. Chem. Interfacial Electrochem. 26 (1970) 1–11, https://doi.org/10.1016/S0022-0728(70)80060-2.
[129] T. Kodera, M. Honda, H. Kita, Electrochemical Behaviour of hydrazine on platinum in alkaline solution, Electrochim. Acta 30 (1985) 669–675, https://doi.org/10.1016/0013-4686(85)80110-9.
[130] V. Rosca, M.T.M. Koper, Electrocatalytic oxidation of hydrazine on platinum electrodes in alkaline solutions, Electrochim. Acta 53 (2008) 5199–5205, https://doi.org/10.1016/j.electacta.2008.02.054.
[131] L. Zhang, W. Niu, W. Gao, L. Qi, J. Zhao, M. Xu, G. Xu, Facet-dependent electrocatalytic activities of Pd nanocrystals toward the electro-oxidation of hydrazine, Electrochem. Commun. 37 (2013) 57–60, https://doi.org/10.1016/j.elecom.2013.10.006.
[132] Z. Takehara, A. Yamano, T. Gozen, S. Yoshizawa, Anodic reactions of hydrazine and ammonia in potassium hydroxide solution, DENKI KAGAKU 41 (1973) 36–41.
[133] M.W. Breiter, Electrochemical Processes in Fuel Cells, Springer Berlin Heidelberg, Berlin, Heidelberg, 1969, https://doi.org/10.1007/978-3-642-46155-2.
[134] M. Petek, S. Bruckenstein, An isotopic labeling investigation of the mechanism of the electrooxidation of hydrazine at platinum, J. Electroanal. Chem. Interfacial Electrochem. 47 (1973) 329–333, https://doi.org/10.1016/S0022-0728(73)80458-9.
[135] K. Arnolds, J. Heitbaum, W. Vielstich, Investigations on the rupture of the N-N-bond within the anodic oxidation and catalytic decomposition of hydrazine, Z. Für Naturforsch. A. 29 (1974) 359–362, https://doi.org/10.1515/zna-1974-0229.
[136] D.J. Alberas, J. Kiss, Z.-M. Liu, J.M. White, Surface chemistry of hydrazine on Pt (111), Surf. Sci. 278 (1992) 51–61, https://doi.org/10.1016/0039-6028(92)90583-R.
[137] M.K. Agusta, W.A. Diño, M. David, H. Nakanishi, H. Kasai, Theoretical study of hydrazine adsorption on Pt(111): anti or cis? Surf. Sci. 605 (2011) 1347–1353, https://doi.org/10.1016/j.susc.2011.04.029.
[138] J.L. Gland, G.B. Fisher, G.E. Mitchell, Vibrational characterization of adsorbed NH on the Ni(111) surface, Chem. Phys. Lett. 119 (1985) 89–92, https://doi.org/10.1016/0009-2614(85)85426-9.
[139] R.T. Rewick, B.J. Wood, H. Wise, Metal catalysis. I: properties of Al2O3 supported Ir/Ni for hydrazine decompositionle, J. Phys. Chem. 83 (1979) 2480–2485.
[140] X. Lin, H. Wen, D.-X. Zhang, G.-X. Cao, P. Wang, Highly dispersed nickel nitride nanoparticles on nickel nanosheets as an active catalyst for hydrazine electrooxidation, J. Mater. Chem. A. 8 (2020) 632–638, https://doi.org/10.1039/C9TA11023B.
[141] M.K. Agusta, H. Kasai, First principles investigations of hydrazine adsorption conformations on Ni(111) surface, Surf. Sci. 606 (2012) 766–771, https://doi.org/10.1016/j.susc.2012.01.009.

[142] A.G. Oshchepkov, A. Bonnefont, E.R. Savinova, On the influence of the extent of oxidation on the kinetics of the hydrogen electrode reactions on polycrystalline nickel, Electrocatalysis 11 (2020) 133–142, https://doi.org/10.1007/s12678-019-00560-3.
[143] L.D. Burke, B.H. Lee, An investigation of some electrocatalytic processes occurring at low potentials at a nickel electrode in base, J. Electrochem. Soc. 138 (1991) 2496–2504, https://doi.org/10.1149/1.2086008.
[144] T.-Y. Jeon, M. Watanabe, K. Miyatake, Carbon segregation-induced highly metallic Ni nanoparticles for electrocatalytic oxidation of hydrazine in alkaline media, ACS Appl. Mater. Interfaces 6 (2014) 18445–18449, https://doi.org/10.1021/am5058635.
[145] K. Asazawa, K. Yamada, H. Tanaka, M. Taniguchi, K. Oguro, Electrochemical oxidation of hydrazine and its derivatives on the surface of metal electrodes in alkaline media, J. Power Sources 191 (2009) 362–365, https://doi.org/10.1016/j.jpowsour.2009.02.009.
[146] R. Liu, X. Jiang, F. Guo, N. Shi, J. Yin, G. Wang, D. Cao, Carbon fiber cloth supported micro- and nano-structured Co as the electrode for hydrazine oxidation in alkaline media, Electrochim. Acta 94 (2013) 214–218, https://doi.org/10.1016/j.electacta.2013.02.011.
[147] E. Granot, B. Filanovsky, I. Presman, I. Kuras, F. Patolsky, Hydrazine/air direct-liquid fuel cell based on nanostructured copper anodes, J. Power Sources 204 (2012) 116–121, https://doi.org/10.1016/j.jpowsour.2011.12.008.
[148] D.C. de Oliveira, W.O. Silva, M. Chatenet, F.H.B. Lima, NiOx-Pt/C nanocomposites: highly active electrocatalysts for the electrochemical oxidation of hydrazine, Appl. Catal. B Environ. 201 (2017) 22–28, https://doi.org/10.1016/j.apcatb.2016.08.007.
[149] L.Q. Ye, Z.P. Li, H.Y. Qin, J.K. Zhu, B.H. Liu, Hydrazine electrooxidation on a composite catalyst consisting of nickel and palladium, J. Power Sources 196 (2011) 956–961, https://doi.org/10.1016/j.jpowsour.2010.08.089.
[150] M. Sun, Z. Lu, L. Luo, Z. Chang, X. Sun, A 3D porous Ni–Cu alloy film for high-performance hydrazine electrooxidation, Nanoscale 8 (2016) 1479–1484, https://doi.org/10.1039/C5NR07072D.
[151] H. Wang, Y. Ma, R. Wang, J. Key, V. Linkov, S. Ji, Liquid–liquid interface-mediated room-temperature synthesis of amorphous NiCo pompoms from ultrathin nanosheets with high catalytic activity for hydrazine oxidation, Chem. Commun. 51 (2015) 3570–3573, https://doi.org/10.1039/C4CC09928A.
[152] P. Tang, H. Wen, C. Chen, X. Lin, P. Wang, Hierarchically nanostructured (Ni,Co) phosphides for hydrazine electrooxidation, Electrochim. Acta 387 (2021) 138492, https://doi.org/10.1016/j.electacta.2021.138492.
[153] T. Sakamoto, K. Asazawa, J. Sanabria-Chinchilla, U. Martinez, B. Halevi, P. Atanassov, P. Strasser, H. Tanaka, Combinatorial discovery of Ni-based binary and ternary catalysts for hydrazine electrooxidation for use in anion exchange membrane fuel cells, J. Power Sources 247 (2014) 605–611, https://doi.org/10.1016/j.jpowsour.2013.08.107.
[154] Z. Feng, D. Li, L. Wang, Q. Sun, P. Lu, P. Xing, M. An, In situ grown nanosheet Ni Zn alloy on Ni foam for high performance hydrazine electrooxidation, Electrochim. Acta 304 (2019) 275–281, https://doi.org/10.1016/j.electacta.2019.03.017.
[155] Z. Zhang, P. Tang, H. Wen, P. Wang, Bicontinuous nanoporous Ni-Fe alloy as a highly active catalyst for hydrazine electrooxidation, J. Alloy. Compd. 906 (2022) 164370, https://doi.org/10.1016/j.jallcom.2022.164370.
[156] L. He, Y. Huang, X.Y. Liu, L. Li, A. Wang, X. Wang, C.-Y. Mou, T. Zhang, Structural and catalytic properties of supported Ni–Ir alloy catalysts for H2 generation via hydrous hydrazine decomposition, Appl. Catal. B Environ. 147 (2014) 779–788, https://doi.org/10.1016/j.apcatb.2013.10.022.
[157] Y. Men, J. Su, X. Wang, P. Cai, G. Cheng, W. Luo, NiPt nanoparticles supported on CeO2 nanospheres for efficient catalytic hydrogen generation from alkaline solution of hydrazine, Chin. Chem. Lett. 30 (2019) 634–637, https://doi.org/10.1016/j.cclet.2018.11.010.
[158] Y.-P. Qiu, Q. Shi, L.-L. Zhou, M.-H. Chen, C. Chen, P.-P. Tang, G.S. Walker, P. Wang, NiPt nanoparticles anchored onto hierarchical nanoporous N-doped carbon as an efficient catalyst for hydrogen generation from hydrazine monohydrate, ACS Appl. Mater. Interfaces 12 (2020) 18617–18624, https://doi.org/10.1021/acsami.0c03096.
[159] T. Karaca, M. Sevim, Ö. Metin, Facile synthesis of monodisperse copper-platinum alloy nanoparticles and their superb catalysis in the hydrolytic dehydrogenation of ammonia borane and hydrazine borane, ChemCatChem 9 (2017) 4185–4190, https://doi.org/10.1002/cctc.201701023.
[160] R.K. Raman, N.A. Choudhury, A.K. Shukla, A high output voltage direct borohydride fuel cell, Electrochem. Solid-State Lett. 7 (2004) A488, https://doi.org/10.1149/1.1817855.
[161] J.B. Lakeman, A. Rose, K.D. Pointon, D.J. Browning, K.V. Lovell, S.C. Waring, J. A. Horsfall, The direct borohydride fuel cell for UUV propulsion power, J. Power Sources 162 (2006) 765–772, https://doi.org/10.1016/j.jpowsour.2005.07.022.
[162] P.-Y. Olu, A. Zadick, N. Job, M. Chatenet, Anode electrocatalysts for direct borohydride and direct ammonia borane fuel cells. in: Electrocatal. Low Temp. Fuel Cells, Wiley-VCH Verlag GmbH & Co. KGaA, Weinheim, Germany, 2017, pp. 317–346, https://doi.org/10.1002/9783527803873.ch10.
[163] I. Merino-Jiménez, C. Ponce de León, A.A. Shah, F.C. Walsh, Developments in direct borohydride fuel cells and remaining challenges, J. Power Sources 219 (2012) 339–357, https://doi.org/10.1016/j.jpowsour.2012.06.091.
[164] Z. Wang, J. Parrondo, C. He, S. Sankarasubramanian, V. Ramani, Efficient pH-gradient-enabled microscale bipolar interfaces in direct borohydride fuel cells, Nat. Energy 4 (2019) 281–289, https://doi.org/10.1038/s41560-019-0330-5.
[165] Z. Wang, M. Mandal, S. Sankarasubramanian, G. Huang, P.A. Kohl, V.K. Ramani, Influence of water transport across microscale bipolar interfaces on the performance of direct borohydride fuel cells, ACS Appl. Energy Mater. 3 (2020) 4449–4456, https://doi.org/10.1021/acsaem.0c00145.
[166] M. Chatenet, Tailoring membranes, Nat. Energy 4 (2019) 261–262.
[167] X. Yang, Y. Liu, S. Li, X. Wei, L. Wang, Y. Chen, A direct borohydride fuel cell with a polymer fiber membrane and non-noble metal catalysts, Sci. Rep. 2 (2012) 567, https://doi.org/10.1038/srep00567.
[168] A. Serov, A. Aziznia, P.H. Benhangi, K. Artyushkova, P. Atanassov, E. Gyenge, Borohydride-tolerant oxygen electroreduction catalyst for mixed-reactant Swiss-roll direct borohydride fuel cells, J. Mater. Chem. A. 1 (2013) 14384, https://doi.org/10.1039/c3ta13457a.
[169] A. Aziznia, C.W. Oloman, E.L. Gyenge, Experimental advances and preliminary mathematical modeling of the Swiss-roll mixed-reactant direct borohydride fuel cell, J. Power Sources 265 (2014) 201–213, https://doi.org/10.1016/j.jpowsour.2014.04.037.
[170] N.Da Mota, D.A. Finkelstein, J.D. Kirtland, C.A. Rodriguez, A.D. Stroock, H. D. Abruña, Membraneless, room-temperature, direct borohydride/cerium fuel cell with power density of over 0.25 W/cm 2, J. Am. Chem. Soc. 134 (2012) 6076–6079, https://doi.org/10.1021/ja211751k.
[171] R. Jamard, J. Salomon, A. Martinent-Beaumont, C. Coutanceau, Life time test in direct borohydride fuel cell system, J. Power Sources 193 (2009) 779–787, https://doi.org/10.1016/j.jpowsour.2009.03.057.
[172] N.A. Choudhury, J. Ma, Y. Sahai, High performance and eco-friendly chitosan hydrogel membrane electrolytes for direct borohydride fuel cells, J. Power Sources 210 (2012) 358–365, https://doi.org/10.1016/j.jpowsour.2012.03.013.
[173] Z. Wang, S. Sankarasubramanian, V. Ramani, Reactant-transport engineering approach to high-power direct borohydride fuel cells, Cell Rep. Phys. Sci. 1 (2020) 100084, https://doi.org/10.1016/j.xcrp.2020.100084.
[174] G. Braesch, A.G. Oshchepkov, A. Bonnefont, F. Asonkeng, T. Maurer, G. Maranzana, E.R. Savinova, M. Chatenet, Nickel 3D structures enhanced by electrodeposition of nickel nanoparticles as high performance anodes for direct borohydride fuel cells, ChemElectroChem 7 (2020) 1789–1799, https://doi.org/10.1002/celc.202000254.
[175] D.A. Finkelstein, J.D. Kirtland, N.Da Mota, A.D. Stroock, H.D. Abruña, Alternative oxidants for high-power fuel cells studied by rotating disk electrode (RDE) voltammetry at Pt, Au, and glassy carbon electrodes, J. Phys. Chem. C. 115 (2011) 6073–6084, https://doi.org/10.1021/jp1082505.
[176] S. Ould-Amara, J. Dillet, S. Didierjean, M. Chatenet, G. Maranzana, Operating heterogeneities within a direct borohydride fuel cell, J. Power Sources 439 (2019) 227099, https://doi.org/10.1016/j.jpowsour.2019.227099.
[177] B.H. Liu, S. Suda, Influences of fuel crossover on cathode performance in a micro borohydride fuel cell, J. Power Sources 164 (2007) 100–104, https://doi.org/10.1016/j.jpowsour.2006.09.107.
[178] H. Cheng, K. Scott, K. Lovell, Material aspects of the design and operation of direct borohydride fuel cells, Fuel Cells 6 (2006) 367–375, https://doi.org/10.1002/fuce.200500260.
[179] H. Cheng, K. Scott, Investigation of Ti mesh-supported anodes for direct borohydride fuel cells, J. Appl. Electrochem. 36 (2006) 1361–1366, https://doi.org/10.1007/s10800-006-9199-7.
[180] B.H. Liu, Z.P. Li, Current status and progress of direct borohydride fuel cell technology development, J. Power Sources 187 (2009) 291–297, https://doi.org/10.1016/j.jpowsour.2008.11.017.
[181] M. Chatenet, F. Micoud, I. Roche, E. Chainet, J. Vondrák, Kinetics of sodium borohydride direct oxidation and oxygen reduction in sodium hydroxide electrolyte, Electrochim. Acta 51 (2006) 5452–5458, https://doi.org/10.1016/j.electacta.2006.02.014.
[182] A.C. Garcia, F.H.B. Lima, E.A. Ticianelli, M. Chatenet, Carbon-supported nickel-doped manganese oxides as electrocatalysts for the oxygen reduction reaction in the presence of sodium borohydride, J. Power Sources 222 (2013) 305–312, https://doi.org/10.1016/j.jpowsour.2012.08.049.
[183] Z.P. Li, B.H. Liu, K. Arai, S. Suda, A fuel cell development for using borohydrides as the fuel, J. Electrochem. Soc. 150 (2003) A868, https://doi.org/10.1149/1.1576767.
[184] H. Cheng, K. Scott, Influence of operation conditions on direct borohydride fuel cell performance, J. Power Sources 160 (2006) 407–412, https://doi.org/10.1016/j.jpowsour.2006.01.097.
[185] Z.P. Li, Z.X. Liu, H.Y. Qin, K.N. Zhu, B.H. Liu, Performance degradation of a direct borohydride fuel cell, J. Power Sources 236 (2013) 17–24, https://doi.org/10.1016/j.jpowsour.2013.01.175.
[186] P.-Y. Olu, F. Deschamps, G. Caldarella, M. Chatenet, N. Job, Investigation of platinum and palladium as potential anodic catalysts for direct borohydride and ammonia borane fuel cells, J. Power Sources 297 (2015) 492–503, https://doi.org/10.1016/j.jpowsour.2015.08.022.
[187] A. Zadick, L. Dubau, N. Sergent, G. Berthomé, M. Chatenet, Huge instability of Pt/C catalysts in alkaline medium, ACS Catal. 5 (2015) 4819–4824, https://doi.org/10.1021/acscatal.5b01037.
[188] C. Lafforgue, A. Zadick, L. Dubau, F. Maillard, M. Chatenet, Selected review of the degradation of Pt and Pd-based carbon-supported electrocatalysts for alkaline fuel cells: towards mechanisms of degradation, Fuel Cells 18 (2018) 229–238, https://doi.org/10.1002/fuce.201700094.
[189] P.-Y. Olu, N. Job, M. Chatenet, Evaluation of anode (electro)catalytic materials for the direct borohydride fuel cell: methods and benchmarks, J. Power Sources 327 (2016) 235–257, https://doi.org/10.1016/j.jpowsour.2016.07.041.
[190] G. Braesch, Z. Wang, S. Sankarasubramanian, A.G. Oshchepkov, A. Bonnefont, E. R. Savinova, V. Ramani, M. Chatenet, A high performance direct borohydride fuel cell using bipolar interfaces and noble metal-free Ni-based anodes, J. Mater. Chem. A. 8 (2020) 20543–20552, https://doi.org/10.1039/D0TA06405J.

[191] F. Asonkeng, G. Maranzana, J. Proust, M. François, L. Le Joncour, J. Dillet, S. Didierjean, G. Braesch, M. Chatenet, T. Maurer, Synthesis of metallic nanoparticles for heterogeneous catalysis: application to the Direct Borohydride Fuel Cell, Appl. Catal. A Gen. 618 (2021) 118117, https://doi.org/10.1016/j.apcata.2021.118117.
[192] M. Abdolmaleki, M.G. Hosseini, A development in direct borohydride/hydrogen peroxide fuel cell using nanostructured Ni-Pt/C anode, Fuel Cells 17 (2017) 321–327, https://doi.org/10.1002/fuce.201600134.
[193] C. Ponce de León, A. Kulak, S. Williams, I. Merino-Jiménez, F.C. Walsh, Improvements in direct borohydride fuel cells using three-dimensional electrodes, Catal. Today 170 (2011) 148–154, https://doi.org/10.1016/j.cattod.2011.03.010.
[194] A.A. Abahussain, C.P. de Leon, F.C. Walsh, Mass-transfer measurements at porous 3D Pt-Ir/Ti electrodes in a direct borohydride fuel cell, J. Electrochem. Soc. 165 (2018) F198–F206, https://doi.org/10.1149/2.0751803jes.
[195] R.M.E. Hjelm, C. Lafforgue, R.W. Atkinson, Y. Garsany, R.O. Stroman, M. Chatenet, K. Swider-Lyons, Impact of the anode catalyst layer design on the performance of H 2 O 2 -direct borohydride fuel cells, J. Electrochem. Soc. 166 (2019) F1218–F1228, https://doi.org/10.1149/2.0681914jes.
[196] F.M. Auxilia, T. Tanabe, S. Ishihara, G. Saravanan, G.V. Ramesh, F. Matsumoto, X. Ya, K. Ariga, A. Dakshanamoorthy, H. Abe, Interleaved mesoporous copper for the anode catalysis in direct ammonium borane fuel cells, J. Nanosci. Nanotechnol. 14 (2014) 4443–4448, https://doi.org/10.1166/jnn.2014.8278.
[197] Y. Zhang, G. Zhu, Z. Chen, Y. Liu, D. Ye, A. Wang, W. Jiang, C. Deng, X. Zhuang, J. Zhang, C. Ke, Direct hydrazine borane fuel cells using non-noble carbon-supported polypyrrole cobalt hydroxide as an anode catalyst, Sustain. Energy Fuels. 7 (2023) 2594–2600, https://doi.org/10.1039/D3SE00329A.
[198] K. Tamura, T. Kahara, Exhaust gas compositions and fuel efficiencies of hydrazine-air fuel cells, J. Electrochem. Soc. 123 (1976) 776–780, https://doi.org/10.1149/1.2132932.
[199] H. Tanaka, K. Asazawa, T. Sakamoto, T. Kato, M. Kai, S. Yamaguchi, K. Yamada, H. Fujikawa, Platinum-free anionic fuel cells for automotive applications, ECS Trans. 16 (2008) 459–464, https://doi.org/10.1149/1.2981880.
[200] A. Serov, M. Padilla, A.J. Roy, P. Atanassov, T. Sakamoto, K. Asazawa, H. Tanaka, Anode catalysts for direct hydrazine fuel cells: from laboratory test to an electric vehicle, Angew. Chem. Int. Ed. 53 (2014) 10336–10339, https://doi.org/10.1002/anie.201404734.
[201] K. Yamada, K. Yasuda, N. Fujiwara, Z. Siroma, H. Tanaka, Y. Miyazaki, T. Kobayashi, Potential application of anion-exchange membrane for hydrazine fuel cell electrolyte, Electrochem. Commun. 5 (2003) 892–896, https://doi.org/10.1016/j.elecom.2003.08.015.
[202] H. Qin, Z. Liu, Y. Guo, Z. Li, The affects of membrane on the cell performance when using alkaline borohydride–hydrazine solutions as the fuel, Int. J. Hydrog. Energy 35 (2010) 2868–2871, https://doi.org/10.1016/j.ijhydene.2009.05.004.
[203] K. Yamada, K. Yasuda, H. Tanaka, Y. Miyazaki, T. Kobayashi, Effect of anode electrocatalyst for direct hydrazine fuel cell using proton exchange membrane, J. Power Sources 122 (2003) 132–137, https://doi.org/10.1016/S0378-7753(03)00440-3.
[204] K. Asazawa, T. Sakamoto, S. Yamaguchi, K. Yamada, H. Fujikawa, H. Tanaka, K. Oguro, Study of anode catalysts and fuel concentration on direct hydrazine alkaline anion-exchange membrane fuel cells, J. Electrochem. Soc. 156 (2009) B509, https://doi.org/10.1149/1.3082129.
[205] K. Asazawa, K. Yamada, H. Tanaka, A. Oka, M. Taniguchi, T. Kobayashi, A platinum-free zero-carbon-emission easy fuelling direct hydrazine fuel cell for vehicles, Angew. Chem. 119 (2007) 8170–8173, https://doi.org/10.1002/ange.200701334.
[206] T. Sakamoto, K. Asazawa, K. Yamada, H. Tanaka, Study of Pt-free anode catalysts for anion exchange membrane fuel cells, Catal. Today 164 (2011) 181–185, https://doi.org/10.1016/j.cattod.2010.11.012.
[207] T. Sakamoto, D. Matsumura, K. Asazawa, U. Martinez, A. Serov, K. Artyushkova, P. Atanassov, K. Tamura, Y. Nishihata, H. Tanaka, Operando XAFS study of carbon supported Ni, NiZn, and Co catalysts for hydrazine electrooxidation for use in anion exchange membrane fuel cells, Electrochim. Acta 163 (2015) 116–122, https://doi.org/10.1016/j.electacta.2015.02.156.
[208] U. Martinez, S. Rojas-Carbonell, B. Halevi, K. Artyushkova, B. Kiefer, T. Sakamoto, K. Asazawa, H. Tanaka, A. Datye, P. Atanassov, Ni-La electrocatalysts for direct hydrazine alkaline anion-exchange membrane fuel cells, J. Electrochem. Soc. 161 (2014) H3106–H3112, https://doi.org/10.1149/2.0191413jes.
[209] M.G. Hosseini, R. Mahmoodi, M. Abdolmaleki, High performance direct hydrazine–hydrogen peroxide fuel cell using reduced graphene oxide supported Ni@M (M = Pt, Pd, Ru) nanoparticles as novel anodic electrocatalysts, N. J. Chem. 42 (2018) 12222–12233, https://doi.org/10.1039/C8NJ00863A.
[210] R. Crisafulli, D.F. de Paula, S.C. Zignani, L. Spadaro, A. Palella, S. Boninelli, J. A. Dias, J.J. Linares, Promoting effect of Cu on Pd applied to the hydrazine electro-oxidation and direct hydrazine fuel cells, Catalysts 12 (2022) 1639, https://doi.org/10.3390/catal12121639.
[211] M.G. Hosseini, V. Daneshvari-Esfahlan, H. Aghajani, S. Wolf, V. Hacker, Palladium-nickel electrocatalysts on nitrogen-doped reduced graphene oxide nanosheets for direct hydrazine/hydrogen peroxide fuel cells, Catalysts 11 (2021) 1372, https://doi.org/10.3390/catal11111372.
[212] Z. Lu, M. Sun, T. Xu, Y. Li, W. Xu, Z. Chang, Y. Ding, X. Sun, L. Jiang, Superaerophobic electrodes for direct hydrazine fuel cells, Adv. Mater. 27 (2015) 2361–2366, https://doi.org/10.1002/adma.201500064.
[213] K. Akbar, J.H. Kim, Z. Lee, M. Kim, Y. Yi, S.-H. Chun, Superaerophobic graphene nano-hills for direct hydrazine fuel cells, e378–e378, NPG Asia Mater. 9 (2017), https://doi.org/10.1038/am.2017.55.
[214] W.X. Yin, Z.P. Li, J.K. Zhu, H.Y. Qin, Effects of NaOH addition on performance of the direct hydrazine fuel cell, J. Power Sour. 182 (2008) 520–523, https://doi.org/10.1016/j.jpowsour.2008.04.028.
[215] Y.S. Kim, B. Kim, T.Y. Jeong, N.H. Kim, E. Ko, J.W. Bae, C.-H. Chung, The development of a gas-feeding CO_2 fuel cell using direct hydrazine oxidation reaction, J. CO_2 Util. 73 (2023) 102527, https://doi.org/10.1016/j.jcou.2023.102527.
[216] D.A. Finkelstein, E. Bertin, S. Garbarino, D. Guay, Mechanistic similarity in catalytic N 2 production from NH 3 and NO 2 – at Pt(100) thin films: toward a universal catalytic pathway for simple N-containing species, and its application to in situ removal of NH 3 poisons, J. Phys. Chem. C. 119 (2015) 9860–9878, https://doi.org/10.1021/acs.jpcc.5b00949.
[217] A.G. Oshchepkov, G. Braesch, A. Bonnefont, E.R. Savinova, M. Chatenet, Recent advances in the understanding of nickel-based catalysts for the oxidation of hydrogen-containing fuels in alkaline media, ACS Catal. 10 (2020) 7043–7068, https://doi.org/10.1021/acscatal.0c00101.